THESIS FOR THE DEGREE OF DOCTOR OF PHILOSOPHY

Highly Concentrated Electrolytes for Rechargeable Lithium Batteries

VIKTOR NILSSON

CHALMERS

UPPSALA
UNIVERSITET

Department of Physics
CHALMERS UNIVERSITY OF TECHNOLOGY
Göteborg, Sweden 2020

Highly Concentrated Electrolytes for Rechargeable Lithium Batteries
VIKTOR NILSSON
ISBN 978-91-7905-260-7

Doktorsavhandlingar vid Chalmers tekniska högskola
Ny serie nr 4727
ISSN 0346-718X

Department of Physics
Chalmers University of Technology
SE-412 96 Göteborg
Sweden
Telephone + 46 (0)31-772 1000

This thesis is for a double degree at Chalmers University of Technology and Uppsala University.

This work has been funded by ALISTORE – European Research Institute and by the Swedish Energy Agency through “Batterifonden” grant 39042-1.

Chalmers, Reproservice
Göteborg, Sweden 2020

UPPSALA
UNIVERSITET

Digital Comprehensive Summaries of Uppsala Dissertations from the Faculty of Science and Technology 1913

Highly Concentrated Electrolytes for Rechargeable Lithium Batteries

VIKTOR NILSSON

ACTA
UNIVERSITATIS
UPSALIENSIS
UPPSALA
2020

ISSN 1651-6214
urn:nbn:se:uu:diva-406483

Dissertation presented at Uppsala University to be publicly examined in PJ-salen, Fysikgården 2B, Göteborg, Wednesday, 8 April 2020 at 13:00 for the degree of Doctor of Philosophy. The examination will be conducted in English. Faculty examiner: Professor Serena Corr (The University of Sheffield).

Abstract
Nilsson, V. 2020. Highly Concentrated Electrolytes for Rechargeable Lithium Batteries. *Digital Comprehensive Summaries of Uppsala Dissertations from the Faculty of Science and Technology* 1913. 61 pp. Uppsala: Acta Universitatis Upsaliensis.

The electrolyte is a crucial part of any lithium battery, strongly affecting longevity and safety. It has to survive rather severe conditions, not the least at the electrode/electrolyte interfaces. Current commercial electrolytes are almost all based on 1 M $LiPF_6$ in a mixture of organic solvents and while these balance the many requirements of the cells, they are volatile and degrade at temperatures above ca. 70°C. The salt could potentially be replaced with e.g. LiTFSI, but dissolution of the Al current collector would be an issue. Replacing the graphite electrode by Li metal, for large gains in energy density, challenges the electrolyte further by exposing it to freshly deposited Li, leading to poor coulombic efficiency and consumption of both Li and electrolyte. Highly concentrated electrolytes (HCEs) have emerged as a possible remedy to all of the above, by a changed solvation structure where all solvent molecules are coordinated to cations – leading to a lowered volatility, a reduced Al dissolution, and higher electrochemical stability, at the expense of higher viscosity and lower ionic conductivity.

In this thesis both the fundamentals and various approaches to application of HCEs to lithium batteries are studied. First, LiTFSI–acetonitrile electrolytes of different salt concentrations were studied with respect to electrochemical stability, including chemical analysis of the passivating solid electrolyte interphases (SEIs) on the graphite electrodes. However, some problems with solvent reduction remained, why second, LiTFSI–ethylene carbonate (EC) HCEs were employed vs. Li metal electrodes. Safety was improved by avoiding volatile solvents and compatibility with polymer separators was proven, making the HCE practically useful. Third, the transport properties of HCEs were studied with respect to salt solvation, viscosity and conductivity, and related to the rate performance of battery cells. Finally, LiTFSI–EC based electrolytes were tested vs. high voltage NMC622 electrodes.

The overall impressive electrochemical stability improvements shown by HCEs do not generally overcome the inherent properties of the constituent parts, and parasitic reactions ultimately leads to cell failure. Furthermore, improvements in ionic transport can not be expected in most HCEs; on the contrary, the reduced conductivity leads to a lower rate capability. Based on this knowledge, turning to a concept of electrolyte compositions where the inherent drawbacks of HCEs are circumvented leads to surprisingly good electrolytes even for Li metal battery cells, and with additives, Al dissolution can be prevented also when using NMC622 electrodes.

Keywords: Li-ion battery, SEI, Highly concentrated electrolyte, Al dissolution, Li metal battery, ion transport

Viktor Nilsson, Department of Chemistry - Ångström, Structural Chemistry, Box 538, Uppsala University, SE-751 21 Uppsala, Sweden.

ISSN 1651-6214
urn:nbn:se:uu:diva-406483 (http://urn.kb.se/resolve?urn=urn:nbn:se:uu:diva-406483)

Highly Concentrated Electrolytes for Rechargeable Lithium Batteries

VIKTOR NILSSON

Department of Physics
Chalmers University of Technology

Department of Chemistry–Ångström Laboratory
Uppsala University

Abstract

The electrolyte is a crucial part of any lithium battery, strongly affecting longevity and safety. It has to survive rather severe conditions, not the least at the electrode/electrolyte interfaces. Current commercial electrolytes are almost all based on 1 M $LiPF_6$ in a mixture of organic solvents and while these balance the many requirements of the cells, they are volatile and degrade at temperatures above ca. 70°C. The salt could potentially be replaced with *e.g.* LiTFSI, but dissolution of the Al current collector would be an issue. Replacing the graphite electrode by Li metal, for large gains in energy density, challenges the electrolyte further by exposing it to freshly deposited Li, leading to poor coulombic efficiency and consumption of both Li and electrolyte. Highly concentrated electrolytes (HCEs) have emerged as a possible remedy to all of the above, by a changed solvation structure where all solvent molecules are coordinated to cations – leading to a lowered volatility, a reduced Al dissolution, and higher electrochemical stability, at the expense of higher viscosity and lower ionic conductivity.

In this thesis both the fundamentals and various approaches to application of HCEs to lithium batteries are studied. First, LiTFSI–acetonitrile electrolytes of different salt concentrations were studied with respect to electrochemical stability, including chemical analysis of the passivating solid electrolyte interphases on the graphite electrodes. However, some problems with solvent reduction remained, why second, LiTFSI–ethylene carbonate (EC) HCEs were employed *vs.* Li metal electrodes. Safety was improved by avoiding volatile solvents and compatibility with polymer separators was proven, making the HCE practically useful. Third, the transport properties of HCEs were studied with respect to salt solvation, viscosity and conductivity, and related to the rate performance of battery cells. Finally, LiTFSI–EC based electrolytes were tested *vs.* high voltage NMC622 electrodes.

The overall impressive electrochemical stability improvements shown by HCEs do not generally overcome the inherent properties of the constituent parts, and parasitic reactions ultimately leads to cell failure. Furthermore, improvements in ionic transport can not be expected in most HCEs; on the contrary, the reduced conductivity leads to a lower rate capability. Based on this knowledge, turning to a concept of electrolyte compositions where the inherent drawbacks of HCEs are circumvented leads to surprisingly good electrolytes even for Li metal battery cells, and with additives, Al dissolution can be prevented also when using NMC622 electrodes.

Keywords: Li-ion battery, SEI, Highly concentrated electrolyte, Al dissolution, Li metal battery, ion transport.

In memory of my grandfather who talked me into academic studies.

List of Papers

This thesis is based on the following papers, which are referred to in the text by their Roman numerals.

I *Critical evaluation of the stability of highly concentrated LiTFSI - acetonitrile electrolytes vs. graphite, lithium metal and $LiFePO_4$ electrodes*
V. Nilsson, R. Younesi, D. Brandell, K. Edström and P. Johansson
J. Power Sources 384 (2018) 334–341.

II *Highly Concentrated LiTFSI–EC Electrolytes for Lithium Metal Batteries*
V. Nilsson, A. Kotronia, M. Lacey, K. Edström and P. Johansson
ACS Appl. Energy Mater 3 (2020) 200-207.

III *Interactions and Transport in LiTFSI-based Highly Concentrated Electrolytes*
V. Nilsson, D. Bernin, D. Brandell, K. Edström and P. Johansson
Accepted for publication in ChemPhysChem.

IV *Additives and Separators for LiTFSI–EC Electrolytes vs. Lithium metal, Graphite and NMC622 Electrodes*
V. Nilsson, P. Johansson, K. Edström and R. Younesi
Manuscript.

Contribution Report

I I planned the work together with my co-authors, performed all analysis and all experiments except for operating the SEM, where I took part. I wrote the manuscript with feedback from my co-authors, finalized it, and responded to reviewers. The sections on SEM and XPS were added during revision and were written solely by me.

II I planned all the work based on my idea, with some suggestions from my co-authors, performed all analysis and experiments except for operating the SEM, where I took part. I wrote the manuscript with feedback from my co-authors, and corresponded with the editor during the revision.

III I planned all the work based on my idea, with some suggestions from my co-authors, performed all analysis and experiments except for running the NMR measurements and analysing NMR data. I wrote the manuscript with feedback from my co-authors.

IV I planned the work based on my idea, performed the experiments and analysis, and wrote the manuscript with minor feedback from my co-authors.

Contents

1 Introduction ... 13
1.1 Scope of the thesis ... 14

2 Batteries ... 15
2.1 Working principles and definitions ... 15
2.2 Cell assembly ... 17
2.3 Electrodes ... 18
2.3.1 Anode materials ... 18
2.3.2 Cathode materials ... 20
2.4 Electrolytes ... 20
2.4.1 The solid electrolyte interphase (SEI) ... 21
2.4.2 Salts ... 22
2.4.3 Solvents ... 22
2.4.4 Ion transport in electrolytes ... 23
2.4.5 Highly concentrated electrolytes (HCEs) ... 24

3 Experimental ... 27
3.1 Materials preparation ... 27
3.2 Physicochemical properties ... 27
3.2.1 Thermal analysis ... 28
3.2.2 Densitometry and viscometry ... 28
3.2.3 Raman spectroscopy ... 29
3.2.4 Pulsed field gradient nuclear magnetic resonance spectroscopy (PFG-NMR) ... 30
3.3 Electrochemical methods ... 30
3.3.1 Reference electrodes ... 31
3.3.2 Battery cell cycling ... 31
3.3.3 Cyclic voltammetry (CV) ... 33
3.3.4 Electrochemical impedance spectroscopy (EIS) ... 33
3.4 *Post mortem* analysis ... 34
3.4.1 X-ray photoelectron spectroscopy (XPS) ... 34
3.4.2 Scanning electron microscopy (SEM) ... 35

4 Results and discussion ... 37
4.1 Re-assessing electrolytes based on inherently unstable components ... 37

4.2 Application of inherently stable electrolytes *vs.* Li metal electrodes 40
4.3 Polymer separators for highly concentrated electrolytes 42
4.4 Ionic transport in highly concentrated electrolytes 43
4.5 Using LiTFSI-EC based electrolytes *vs.* high voltage cathodes 46

5 Concluding remarks and outlook 49

6 Sammanfattning på svenska (Summary in Swedish) 51

7 Acknowledgements 53

1. Introduction

The portable electronics industry was revolutionized by the introduction of the Li-ion battery (LIB) in 1991, and with improvements to the chemistry, manufacturing and cell design over the years, the specific energy has since almost quadrupled to *ca.* 300 Wh/kg [1, 2].[1] We have indeed not seen a comparable development as Moore's law for semiconductors [3], as batteries have fundamentally different limitations imposed by the size, mass and electrochemical potential of the materials used. But the improved batteries have nonetheless led to renewed hopes to reduce our oil dependency, especially in the transportation sector, currently using $>57\,\%$ of all crude oil [4]. Finite oil reserves, local air pollution, and global CO_2 emissions all make substitution of internal combustion engines by electric drivetrains very desirable.

The rapid ongoing vehicle electrification is a major drive for research and development with huge investments in both battery research and production [5]. The technology for light vehicles is already quite mature, but materials availability, cost, and increased energy density with maintained or improved cycle life and safety will allow electrification of new areas, such as heavy duty vehicles, vessels and aircraft. In addition to the transportation sector, there are applications of batteries for load balancing and energy storage in the power grids with high amounts of intermittent solar and wind power. To cater for this demand, alternatives to the LIB such as Li metal (LMB), Li-sulfur (Li-S) and Na-ion (SIB) batteries are being researched.

Lithium batteries are complex systems, for which we do not yet have a full understanding of all reactions and processes at play, especially after modifications to the chemistry [6] or even to the usage pattern. While the energy is stored in the electrodes, their function is tightly dependent on the electrolyte used. Important factors to improve are proper transport properties and electrochemical stability of the electrolyte [7], the adequate formation and stability of the passivation films on the electrode surfaces [8], and the control of slow side-reactions ultimately leading to failure [9].

[1] Two years ago, at the time of my Lic. thesis, the factor was 3.125, today it is 3.75 times the original LIB's 80 Wh/kg.

1.1 Scope of the thesis

This thesis focuses specifically on using *highly concentrated electrolytes* (HCEs) for LIBs and LMBs. The HCEs addresses the aforementioned factors by adding much more salt to the electrolyte, creating a very ion-dense liquid [10]. The studies are performed on two broad kinds of HCEs, those based on inherently stable components, and those where the salt concentration is used to counteract inherent instabilities. Both the fundamental physical and chemical properties, and practical aspects for application are treated: What is the feasibility of highly concentrated electrolytes for lithium batteries and how do we overcome the obstacles that exist? On the more fundamental level, how do the changed coordination structures and transport properties in the bulk relate to the processes at the electrode surfaces?

2. Batteries

In this thesis *battery* refers to the electrochemical cell and not to the battery pack, which is an assembly of cells such as the large battery powering an electric vehicle. Battery and cell are used interchangeably, but battery is exclusively the energy storage device, while cell may refer to other cells for electrochemical experiments.

> Battery: A container consisting of one or more cells, in which chemical energy is converted into electric energy and used as a source of power.
>
> Oxford Dictionary of English [11]

Although much of the following introduction is general, focus is on rechargeable lithium batteries with LIBs and materials used in the appended papers as examples.

2.1 Working principles and definitions

The principle of a battery is to convert chemical energy directly to electricity by separating the electron transfer from a redox reaction. For the example of a typical LIB using a lithium iron phosphate (LFP) cathode, the total reaction of discharge can be written as

$$LiC_6 + FePO_4 \quad \rightarrow \quad C_6 + LiFePO_4 \tag{2.1}$$

where the lithiated graphite anode (LiC_6) is oxidized and the $FePO_4$ cathode is reduced to form $LiFePO_4$.

This reaction can be separated into two half-reactions

$$LiC_6 \quad \rightarrow \quad C_6 + Li^+ + e^- \tag{2.2}$$

$$Li^+ + e^- + FePO_4 \quad \rightarrow \quad LiFePO_4 \tag{2.3}$$

where the (2.2) is the anodic and (2.3) is the cathodic reaction. Now, by physically separating the anode and cathode but connecting them through an external electrical circuit, the electrons are transferred outside of the cell whereas the Li-ions (Li^+) move through the electronically insulating but ionically conducting electrolyte, as illustrated in Fig. 2.1. The anions should ideally not react with the electrodes, they are thus not carrying sustained current and stop moving shortly after the cell is turned on. If the reactions are reversible, as is the case for (Eqn. 2.1), the battery can generally be recharged. Most LIB electrode materials are layered structures where the Li

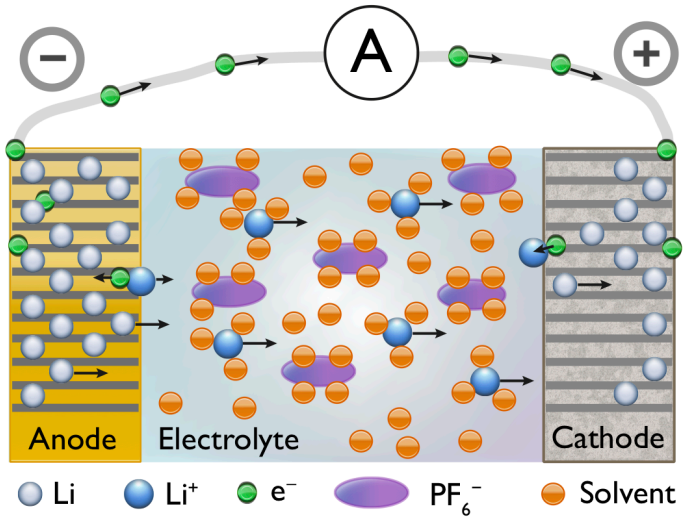

Figure 2.1. A discharging LIB. PF_6^- is the anion of the Li salt.

occupies the space between the layers, roughly maintaining the host structure upon *cycling* (charge and discharge). An insertion process without significant distortion of the structure is called *intercalation*.

The two half-reactions (2.2) and (2.3) have changes in free energy $\Delta G = -nFE$ and corresponding electrochemical potentials E_{an} and E_{cat}, respectively, often measured in V *vs.* Li^+/Li.

The cell voltage is then:

$$E_{cell} = E_{cat} - E_{an}$$

and the energy content of the cell is

$$\int_{0\%}^{100\%} E_{cell}(Q)\, dQ,$$

where the integration is done over the usable capacity Q of the cell, typically determined by *cut-off voltages* for E_{cell}, and where Q is the charge stored in the electrochemically active electrode materials (Fig. 2.2).

The electrolyte has to withstand the potentials of the electrodes, or have a sufficient *electrochemical stability window* (ESW), which is the region between the electrolyte oxidation and reduction potentials, E_{ox} and E_{red}, respectively. The ratio of discharge capacity to charge capacity, $CE = Q_{discharge}/Q_{charge}$, is called *coulombic efficiency* (CE), and measures the chemical reversibility of the cell and is lower than 100% if some charge is lost due to side-reactions.

Traditionally, the *anode* is defined as the electrode where oxidation occurs, whereas the *cathode* is where reduction occurs. A discharging battery is a *galvanic cell* where

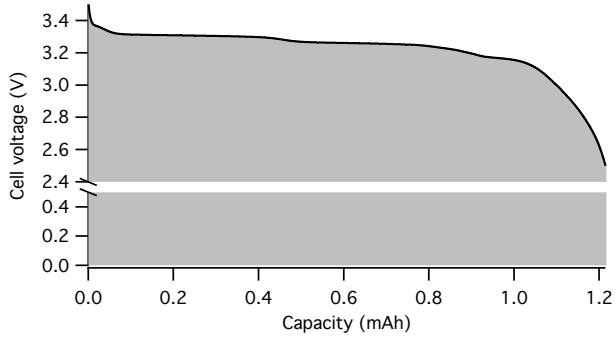

Figure 2.2. A discharge voltage profile with the cell energy illustrated by the shaded area.

the negative electrode is the anode and the positive electrode is the cathode. For the charging cell, the poles should technically switch names, but in most battery literature the electrodes by convention keep their names: anode (−) and cathode (+).

2.2 Cell assembly

The electrochemically active electrode materials are mixed in a slurry with an electronically conductive carbon additive and a polymeric binder, and coated on thin metal foil current collectors. For the cathode, Al foil is used, while the anode must be coated on more expensive and heavy Cu to avoid Al-Li alloying. The foils are coated on both sides and stacked or rolled with a thin polymeric separator between anode and cathode (Fig. 2.3). The cell layout may be described using the notation *graphite*||$LiCoO_2$ or *graphite*|*electrolyte in separator*|$LiCoO_2$. The electrode assembly is placed in a flat or tubular casing, filled with the required amount of electrolyte to wet the electrodes and separator, and then sealed.

Common cell formats in materials research are coin-cells, customised pipe-fittings from Swagelok, and vacuum-sealed pouches. A research cell often uses glass-fibre separators with a thickness of *ca.* 250 µm which is more than 10x that of commercial cells. As a consequence, these cells contain excess electrolyte, which must be taken into account when interpreting the results. These test cells for materials research typically have an electrode diameter in the range of 1–2 cm, and have 1/1000th of the capacity of a cell phone battery or single cylindrical cell — for example, the cells used by Tesla have double-sided electrodes of about 175×6 cm. In early research stages, the benefits of scaling up are small and come with a high cost. However, to get realistic estimates on ageing or rate capabilities, prototype cells are ultimately required. As an example, discharging at short circuit in a 2 mAh coin-cell will only increase the cell temperature with *ca.* 1°C, while a larger cell will reach above 100°C within seconds [12].

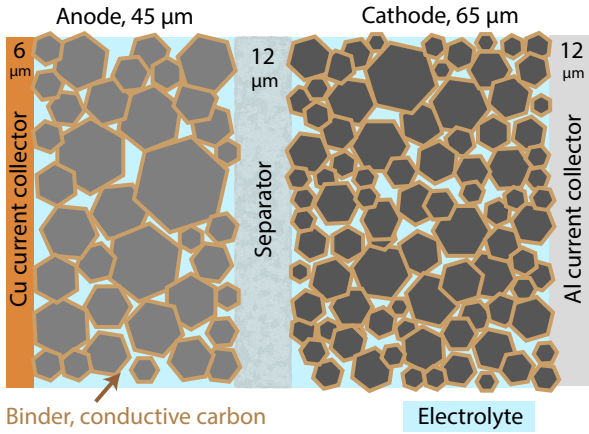

Figure 2.3. A slightly more realistic rendering of a small section of a LIB cell. The thicknesses of foils and separators are typically almost doubled for lab cells.

2.3 Electrodes

Current LIBs almost exclusively use graphite as the anode together with a lithium transition metal oxide cathode. An overview of cathode materials and some alternative anode materials are presented here. [1]

2.3.1 Anode materials

Graphite is used since it offers stable cycling based on its physically and chemically stable structure. Graphite has a theoretical capacity of 372 mAh/g for a LIB, which is calculated directly from the mass of the C_6-unit which hosts one Li. The electrode potential depends on the state of charge (SOC), where stages arise from different phases (Fig. 2.4a). Plateaus are observed in the equilibrium between two phases, *e.g*: $2LiC_6 \rightleftharpoons Li + LiC_6{\cdot}C_6$ at 85 mV for the almost full electrode [13]. The average potential for the graphite anode is ca 0.1 V *vs.* Li^+/Li which gives a high LIB cell voltage.

One alternative to graphite is Si with a theoretical capacity of 3578 mAh/g in the form $Li_{15}Si_4$, and with an electrode potential of ca 0.4 V *vs.* Li^+/Li. However, Si anodes suffer from large volume expansion upon cycling which leads to particle cracking and electrolyte decomposition on the surface [14]. As a remedy, Si is mixed into graphite to create composite electrodes which balance the increased capacity with a limited impact on the stability, and this concept has recently entered the market [15].

[1] Graphite anodes are used in Papers I,IV, Li metal in I,II,IV, LTO in I,III, LFP cathodes in I,III,IV, and NMC in IV.

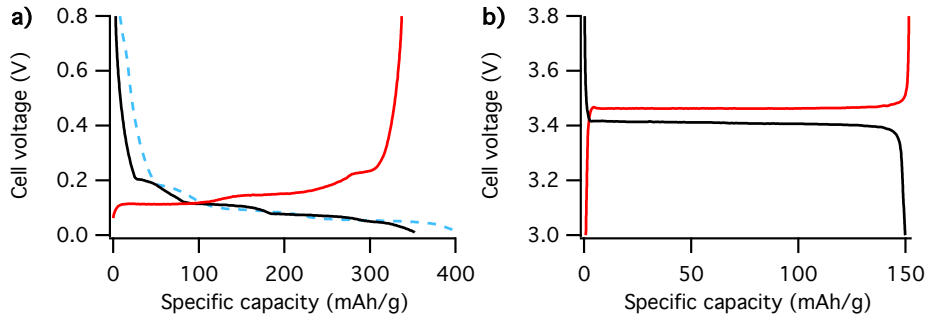

Figure 2.4. Voltage profiles for a) Li | graphite and b) Li | LFP cells. Lithiation is shown with black lines, delithiation with red, and the first graphite lithiation, including more side-reactions of electrode passivation, with dashed blue.

Li has the lowest electrochemical potential of all elements at −3.04 V *vs.* SHE[2] which together with the specific capacity of 3860 mAh/g is the reason why Li is so attractive. Li metal anodes are seen as the "holy grail" of rechargeable Li batteries even though they actually predate the LIB. They were withdrawn from market because of safety issues; dendrites can grow upon charging and penetrate the separator, short-circuiting the cell and causing fire [16]. There are batteries using Li metal anodes on the market, but they rely on solid polymer electrolytes which require operation at elevated temperatures (*ca.* 80°C).

When graphite is replaced by Li metal, the anode capacity increases tenfold. On a cell level, however, the increase is limited to *ca.* 50% since the cathode capacity must be balanced; a significant part of the cell which remains unchanged by the change of anode. With a Li metal anode, the Li is deposited and stripped either directly on the Li metal foil also acting as current collector, or with another current collector such as a Cu foil. In either case, some excess Li is required because of a lower efficiency due to the constant exposure of freshly deposited Li to the electrolyte [17], and furthermore, most cathodes already include the required Li.

Li metal anodes are essential to both Li-S batteries and solid state batteries in order to provide the required energy density on cell level. Furthermore, Li metal is commonly used as a counter electrode in battery research cells because they have a constant potential which is used as a reference, and the Li foil is usually thick, > 100 µm, leading to an overcapacity. Together, this ensures that cell voltage and capacity are governed by the working electrode. Examples of such *half-cells* are shown in Fig. 2.4, where the discharged (low voltage) graphite cell has a graphite electrode in the same state as in a charged *full cell*.

[2]Standard hydrogen electrode is the universal reference in electrochemistry.

Another anode material is lithium titanate, $Li_4Ti_5O_{12}$ (LTO) which in its lithiated state is $Li_7Ti_5O_{12}$ [18]. LTO is used in Papers I & III because of its electrode potential of 1.55 V *vs.* Li^+/Li which is less likely to cause electrolyte reduction. The theoretical specific capacity is only 175 mAh/g which together with the high potential results in a low energy density, but the material offers high rate capability and is therefore useful for high-power applications.

2.3.2 Cathode materials

There is a range of materials to choose from for the cathode, where the layered $LiCoO_2$ (LCO) was used in the original commercialized LIB and is still in use for portable electronics thanks to its high energy density. However, the cycle life and safety are insufficient for automotive applications. A range of analogues to LCO were developed by substituting the problematic Co whereof $LiNi_xMn_yCo_zO_2$, (NMC) is now the most common. Various formulations with $x + y + z = 1$ exist, with more Ni giving higher capacity but lower stability at high voltages and lowered thermal stability [19, 20]. A common drawback for all these materials are that they contain Co, which is toxic, insecure in supply, and connected to child labour [21].

Another cathode, popular for heavy duty applications such as buses, is $LiFePO_4$ (LFP) which has a lower energy density but compensates for this with a high rate (power) capability, long life and low cost [19]. LFP is prepared as carbon-coated nano-sized particles to increase the electronic conductivity. LFP has a voltage plateau at 3.43 V *vs.* Li^+/Li that stretches across the whole capacity window, again a consequence of the equilibrium between two phases in the material (Fig. 2.4b). The relatively low voltage allowed LFP to be used in Papers I-III without causing electrolyte oxidation . The stability of the voltage is exploited when using LFP as a reference electrode (Paper I), but in LIBs it makes it difficult to determine the electrode SOC from its electrode potential.

2.4 Electrolytes

Important properties of a good liquid electrolyte are high Li^+ conductivity, low viscosity to penetrate the pores of the electrode, ability to wet the separator, inertness towards cell components, a wide liquid temperature range and a wide ESW. Apart from liquid electrolytes there are some other types, notably solid polymer electrolytes and ceramic ion conductors which primarily offer improvements with respect to safety, but suffer from low ionic conductivity and poor electrode contact, respectively. The liquid electrolytes are typically salts in aprotic organic solvents, but research is also done on ionic liquid and aqueous electrolytes.

The state of the art electrolyte in LIBs is 1 M $LiPF_6$ in a mixture of the cyclic ethylene carbonate (EC) with a linear carbonate, usually diethyl carbonate (DEC), dimethyl carbonate (DMC) or ethyl methyl carbonate (EMC) [22]. This formulation balances various requirements in the cell well but has drawbacks such as limited stability at elevated temperatures [22] or when combined with high voltage cathodes [23]. In particular, these electrolytes form effective passivating films on the graphite anode and the Al current collector.

2.4.1 The solid electrolyte interphase (SEI)

Since the electrochemical potentials of the anode materials are very low, they are strongly reducing, which few solvents and salts can withstand. However, in the widely used electrolytes, a passivating film forms from the reduced electrolyte species, preventing further electrolyte reduction similar to how aluminium in air is protected by its surface oxide [8]. This passivating film, the solid electrolyte interphase (SEI) [24], is thus a crucial "component" in the LIB. The composition and morphology of it must be investigated to understand the effect of modifications to the electrode and electrolyte chemistry. Conditions for a effective SEI is that it is: electronically insulating (or the reduction will continue on the surface of the film), ionically conducting (to let Li^+ through and not kill the cell), insoluble in the electrolyte, dense and flexible to follow volume changes in the electrode and thermally stable [25].

EC is included in the electrolyte since it forms an effective SEI on graphite [26]. The problem with many other solvents is that they *co-intercalate* with Li^+ without leaving the solvation shell, and cause graphite exfoliation. EC on the other hand, readily reduces on the anode at a higher potential than Li intercalation or decomposition of other components. In addition to this EC reduction, the salt will also decompose; in particular the very stable LiF is formed from electrochemical salt decomposition [7]. Altogether the SEI is a mix of polycrystalline, amorphous and polymeric phases that make up a 10–100 nm film covering the anode [8]. Furthermore, additives such as vinylene carbonate are often included in the electrolyte to improve the SEI [7].

Apart from efforts to form an "artificial" SEI before cell assembly [8], the SEI is formed in the cell. Some reactions occur spontaneously but many take place during the first charge, in the *formation cycle* as illustrated in Fig. 2.4 by the higher capacity required for the first lithiation.

The cathode may also have a passivating film, called the cathode electrolyte interphase (CEI), but it is thin in comparison to the SEI. Formation of both SEI and CEI can furthermore be affected by crosstalk between the electrodes where decomposition products from one deposit on the other [27].

2.4.2 Salts

Before the commercialization of LIBs using $LiPF_6$, the structurally similar $LiAsF_6$ and $LiClO_4$ salts were widely used in research, but were later discarded because of toxicity and risk of explosions, respectively. $LiBF_4$ was also used in early commercial cells, but ultimately $LiPF_6$ turned out to best meet the requirements, especially having a higher ionic conductivity of the electrolyte. $LiPF_6$ is a compromise, however, with respect to its limited thermal stability [28] and sensitivity to hydrolysis [29]. These salts all have pseudo-spherical anions with a central metal coordination centre.

Many new salts have been developed in attempts to replace $LiPF_6$ [7, 30], *e.g.* the sulfonimides LiFSI, LiTFSI and LiBETI (Fig. 2.5), with especially the former two being amongst the most researched salts for new electrolytes. These big and flexible anions do not tend to form crystalline complexes with solvents as easily as PF_6^- does, and the salts dissociate easily which allows for much higher concentrations [31, 32]. They also significantly improve the thermal stability and lower the sensitivity to moisture [33, 34]. A drawback of these salts is dissolution of the Al current collector generally observed for cathode potentials above 3.7 V *vs.* Li^+/Li for LiTFSI and 4.6 V *vs.* Li^+/Li for LiBETI [35]. However, the Al dissolution potential is raised in combination with nitrile solvents [35], which is also seen in Paper I for high salt concentrations. LiFSI gives a higher electrolyte conductivity and may even avoid the Al dissolution, but availability of highly pure salt has been an issue and it is overall less stable [34, 36, 37].

$LiNO_3$ has a very low solubility in most solvents, and is not used as the main salt, but is an important additive for Li-S batteries. In all Papers I–IV, LiTFSI was used as the main electrolyte salt, with $LiPF_6$, $LiBF_4$, and $LiNO_3$ used as additives in papers II & IV.

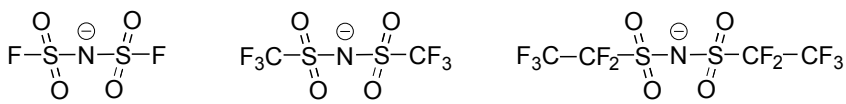

Figure 2.5. Sulfonimide anions.

2.4.3 Solvents

In order to avoid hydrogen evolution, the solvents for Li battery electrolytes are aprotic, and to dissolve the salt they must be polar, excluding many common organic solvents. Most used in early battery research was propylene carbonate (PC), which however never allowed for lithiation of graphite because of severe graphite exfoliation. The structurally similar EC (Fig. 2.6) has a high melting point at 36°C, *vs.* –49°C for

PC, whereas its mixtures with linear carbonates (DMC/DEC/EMC) has liquid ranges to well below room temperature [22].

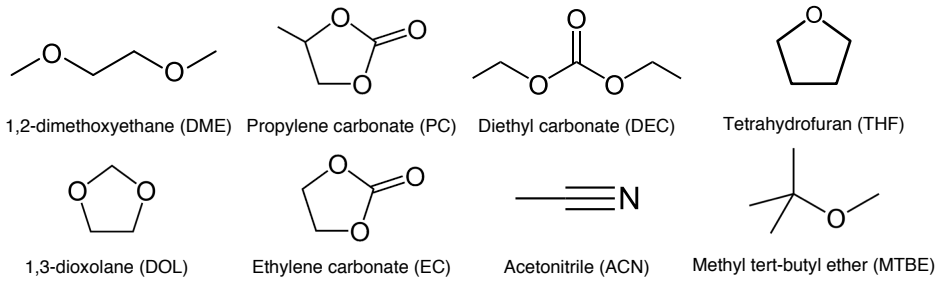

Figure 2.6. The electrolyte solvents used in this thesis.

Acetonitrile (ACN) is widely used in supercapacitors due to its low viscosity and high permittivity (polarity) [38] and is also a common solvent for general non-aqueous electrochemistry. Drawbacks of ACN are that it suffers from a narrow ESW, especially poor reductive stability and inability to form an effective SEI, as seen in Paper I. Furthermore, it forms toxic cyanides when degraded and ACN-based supercapacitors are even forbidden in Japan [38].

LiTFSI in a mix of the cyclic ether dioxolane (DOL) and dimethoxyethane (DME) is the by far most common used electrolyte for Li-S batteries [39] where one of the major problems is the Li metal stability. The DME is a glyme which has multidentate binding to the ions, and is effectively dissolving even $LiNO_3$. Such an electrolyte is used as a reference in Paper II.

2.4.4 Ion transport in electrolytes

The ionic conductivity (σ) of the electrolyte is an important factor for the internal cell resistance and power capability of a LIB. The ionic conductivity in a very dilute electrolyte is low due to the low number of charge carriers. As the salt concentration increases the ionic conductivity will initially follow, while the ion-ion interactions and replaced volume of the electrolyte lead to an increased electrolyte viscosity and decreased ion mobility. Furthermore, ion-pairing and aggregation leads to neutral species in the electrolyte which also decrease the ionic conductivity. The balance between these factors lead to an ionic conductivity with a non-monotonous and non-trivial dependence on salt concentration, but which for common solvents and Li-salts have a maximum around 1 M.

The ionic conductivity is not the only factor determining rate performance of LIBs. The Li^+ transference number, t_+, is the fraction of conductivity carried by Li^+, with an effective electrolyte conductivity given by the product $\sigma \times t_+$. The conduction of anions will form a salt concentration gradient in the cell since the electrodes are

anion-blocking, but they still respond to the electric field. This gradient increases the cell resistance, and salt depletion or precipitation at the electrodes can result. If the anions are immobile, $t_+ \approx 1$, and a smaller concentration gradient will form with in the cell, which is another benefit of high transport numbers.

The transference number is unfortunately quite complicated to measure accurately [40, 41]. Using diffusion measurements, the transport number can be estimated as the ratio of self diffusion coefficients, $t_+ = \frac{D_+}{D_+ + D_-}$, but this requires a completely dissociated electrolyte for the values to represent the true transference number.

> In spite of the very important role that the transference numbers of electrolytes have played in chemical theory, since Hittorf developed sixty years ago the method of determining these quantities by analysis of the electrode solutions, few really accurate transference numbers have been obtained.
>
> Gilbert N. Lewis, 1910 [42]

2.4.5 Highly concentrated electrolytes (HCEs)

Highly concentrated, *superconcentrated*, or *solvent-in-salt* electrolytes, HCEs, have significantly higher salt concentrations than 1 M — already a rather high concentration in many other areas of science (Fig. 2.7).

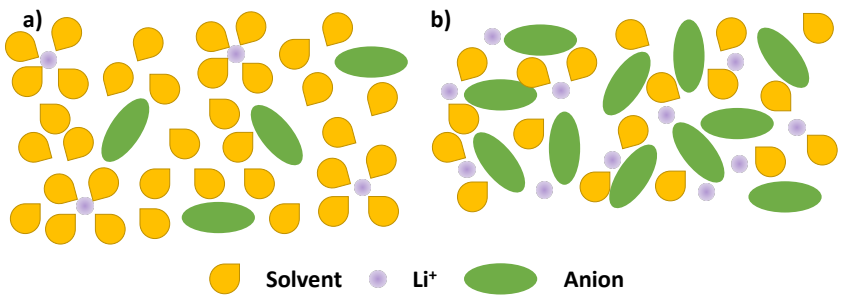

Figure 2.7. Schematic picture of a) *ca.* 1 M electrolyte, and b) an HCE.

Some key points that make these electrolytes special [10]:

- A low amount of solvent, especially in free, non-solvating form.
- An extremely high ion density, which makes it similar to an ionic liquid.
- Higher density, higher viscosity, and lower total ionic conductivity.

Some interesting benefits are observed for HCEs, such as lower solubility of transition metals dissolving from cathodes [43], higher rate capabilities [44], and widened ESWs [45]. The main drawbacks are costs from increased salt use and poor wetting of electrodes and separator.

Research on highly concentrated electrolytes traces back to 1985, when a saturated $LiAsF_6$–PC electrolyte was shown to inhibit solvent co-intercalation in the layered

compound ZrS_2 [46]. In 2002 successful Li^+ intercalation into graphite was demonstrated by Jeong *et al.* using a 1:2 LiBETI–PC electrolyte where the corresponding dilute electrolyte (1:8) caused graphite exfoliation [47]. This was attributed to the changed solvation structure of Li^+, where all solvent is coordinated to the ions.

Since 2010, similar experiments have been made by Yamada *et al.* for LiTFSI and LiFSI in various solvents [43, 48–51], showing that cells can operate at a higher or equal rate to a normal 1 M $LiPF_6$ electrolyte despite a lower conductivity. Another finding is that the SEI is formed mainly by anions in these electrolytes. It is notable that these electrolytes are EC-free but still allow reversible intercalation of Li^+ into graphite, which is desirable because of the negative impact EC has on the low-temperature performance and oxidation stability [52]. The increased rate capability observed could arguably be due to other ion transport mechanisms [53] or due to an increased Li^+ transference number [54].

Li metal anodes have also been studied with HCEs. Suppressed dendrite growth and improved cycling efficiency was shown with highly concentrated LiBETI–PC [55]. LiTFSI in DOL:DME (1:1 by vol.) in addition showed a significantly raised transference number and lower solubility of polysulfides with a higher salt concentration in Li-S battery cells [56].

Another property that greatly improves with highly concentrated electrolytes is prevention of dissolution of the Al current collector when using LiTFSI at high electrode potentials, which is treated in Papers I & IV. There is no consensus on the mechanisms for this [57], some options are: lack of solvent to solvate Al^{3+} and blocking of solvent access to the surface [58], a shift of the reaction equilibrium when the vicinity of the electrode gets saturated with Al^{3+} [59], and formation of a LiF film on the Al, like when using 1 M $LiPF_6$ [60].

Finally, the work on LiTFSI–H_2O "water-in-salt" electrolytes (WISEs) by Xu and co-workers claim expansion of the ESW of aqueous electrolytes from 1.2 V to > 3 V [61, 62]. This has spurred derivative work finding WISEs to be viable alternatives for supercapacitors, although the usable ESW seems smaller than previously claimed [63, 64].

3. Experimental

For a fundamental understanding we start by determining the physico-chemical properties of the electrolytes. The nature of batteries as electrochemical storage devices makes electrochemical analysis a central part of determining the properties of a novel electrolyte and also battery cell testing is a crucial method — why this comes second. After cycling, the cell components are investigated *post mortem*. Here follows an introduction to the methods used for all of the above, including practical matters of special importance to this work.

3.1 Materials preparation

Electrolytes and cells were prepared in an Ar-filled glovebox to avoid moisture and, especially for Li metal, reaction with O_2 or N_2. Mixing of electrolytes is straightforward, but HCEs often have a salt volume larger than the final volume, why both salts and solvents were weighed rather than using a volumetric flask. As a consequence, the density must be measured to get the molarity of the electrolytes (n_{salt}/V_{final}). To ensure a low water content, the solvents were dried with molecular sieves and extra dry salts were used.

Only commercial materials were used, but some composite electrodes for Paper I were prepared in the lab. Slurries for electrode coating were made using the active materials graphite and LFP, carbon black, polyvinylidene difluoride (PVdF) binder and the solvent N-methyl-2-pyrrolidone (NMP). The ingredients were thoroughly mixed in a planetary ball-mill. The PVdF was typically added as a 5 wt.% solution in NMP, but mixing of the dry ingredients before NMP addition allows slurry viscosity tuning with maintained composition. The slurries were coated onto Cu (graphite) and Al (LFP) foils using a roll-to-roll coater for maximum film homogeneity. The ultrathin graphite coatings were made in smaller batches with a bar coater.

3.2 Physicochemical properties

Melting and boiling points, as well as density and viscosity, are important both in practice and fundamentally. For studies of ionic association Raman and NMR spectroscopies have been used. Ionic conductivity is treated later (3.3.4).

3.2.1 Thermal analysis

For a comparison of electrolyte boiling points and volatilities, and an absolute upper operation temperature limit, thermogravimetric analysis (TGA) has been used. The TGA instrument consists of a microbalance inside a furnace with a precisely controlled temperature and gas flow, and typically either a temperature ramp (dynamic) or a stepwise temperature (isotherm) is programmed, where the latter is better suited to prove stability at a specific temperature. The output signal is the mass loss as a function of time or temperature. In electrolytes based on volatile solvents and thermally stable LiTFSI, the solvents evaporate more or less completely before decomposition of the salt occurs. When the non-volatile solvents EC or PC are used, or a less stable salt, also other reactions may activate. In Paper II, dynamic TGA is used to illustrate the large difference in boiling points and vapor pressure between electrolytes.

In differential scanning calorimetry (DSC) the heat flux in/out of the sample is recorded during a temperature sweep. This is useful when investigating phase changes, useful *e.g.* when determining the nature of the transitions in the ionic conductivity data of Paper II. As an example, melting of a crystal is an endothermic process, requiring heat input, which gives rise to a peak at the melting point. The melting point gives the lower operation temperature limit of the electrolyte.

3.2.2 Densitometry and viscometry

The densities, required to determine molar concentrations, were measured using the oscillating U-tube method. The sample is filled into a U-tube which is driven by a piezoelectric actuator and resonates at a frequency which shifts depending on the sample density. Using substances of known density such as air and water, the meter can be calibrated, whereby the oscillation frequency gives an accurate reading of the sample density.

The dynamic viscosities were measured with a rolling ball instrument. The sample, with a known density ρ, is filled in a narrow glass capillary together with a metal ball of known density ρ_b. Because of the small and smooth ball, the Reynolds numbers will be low, and the ball will reach a constant speed when the glass tube is inclined. The speed is measured by the time for the ball to roll between the ends. The drag force on the ball is then given by Stokes' law $F_d = 6\pi r\eta v$ where η is the viscosity and v the ball viscosity. Knowing the densities and the inclination, we set $F_d = F_g$, where F_g is the gravitational force acting on the ball, and solve for η.

Both of these methods rely on careful sample filling to avoid bubbles, which for very viscous samples require preheating of both the capillaries and the samples. Viscosity data can give a hint on how well the electrolyte performs, and is here used together with ionic conductivity data to determine the ionicities of the electrolytes in Paper III.

3.2.3 Raman spectroscopy

Raman spectroscopy is an optical method that probes molecular rotations and vibrations through their change of the electron cloud polarizability.[1] Incoming photons of frequency ν are scattered, and typically due to Rayleigh scattering, they leave the sample in some direction with the same frequency. Due to *Raman scattering*, *ca.* 1/1000 of the scattered photons leave the sample with a lower or higher frequency, $\nu - \Delta\nu$ or $\nu + \Delta\nu$, following the *Stokes* or *anti-Stokes* process, respectively. Stokes scattering occurs when some energy is absorbed by exciting the molecule, while anti-Stokes is energy transfer to the photon from an already excited (virtual) state. Since most states are not excited at room temperature, the Stokes shift (redshift) gives a stronger signal.

The spectrometer uses a monochromatic laser source and a notch filter to suppress the laser wavelength. For dispersive spectrometers, laser lines in the visible spectrum are used, which often results in fluorescent background from presence of even miniscule amounts of impurities in the sample, because fluorescence happens much more frequently than Raman scattering. This is a problem for our electrolytes, why as a remedy, Fourier-transformation Raman spectroscopy (FT-Raman) was used. In FT-Raman the laser wavelength is 1064 nm (IR), which is a low enough energy as not to excite the electronic states of the fluorescing molecules (Fig. 3.1). A drawback is much longer acquisition times, since the Raman scattering intensity is proportional to ν^4.

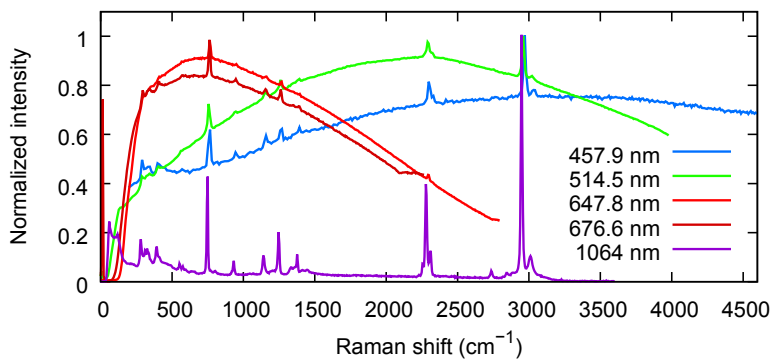

Figure 3.1. Raman spectra using different laser wavelengths.

Some of the vibrational modes give rise to isolated peaks that can be straightforwardly analysed. An example is the TFSI "all breathing mode" at 740 cm^{-1} [65], which shifts to higher wavenumbers when coordinating to Li, and is used to study the local coordination in Paper III.

[1] IR spectroscopy is a complementary technique that sometimes probe the same vibrational modes, but depending on molecular symmetry a mode can be visible exclusively in one of them (or neither).

3.2.4 Pulsed field gradient nuclear magnetic resonance spectroscopy (PFG-NMR)

In NMR spectroscopy, the sample is placed in a narrow glass tube, which is then placed vertically along the z axis inside a large electromagnet. Atoms with non-zero nuclear spins have a magnetic moment which will align with and precess around the z-axis of the external magnetic field B_0. This precession at the *Larmor frequency*, dependent on B_0 and the nuclear mass and spin, will resonate with electromagnetic pulses passed through the sample and can be detected. This is done in time domain by sending a pulse with a component orthogonal to B_0, which is then Fourier transformed to the frequency domain. Just as for XPS (3.4.1), chemical shifts of peaks are in NMR used to identify bonds and their chemical surrounding in a molecule, such as for ^{1}H atoms of THF, which are shifted differently depending if they are close to the oxygen (Fig. 3.2).

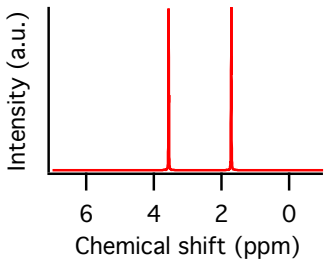

Figure 3.2. ^1H-NMR spectrum for THF in one of the electrolytes.

In this work, we used PFG-NMR in Paper III for measurements of diffusion in electrolytes. In PFG-NMR [66], electromagnetic pulses with a field strength gradient in the z-axis are applied during the measurement. The diffusion leads to a loss of magnetization and hence peak integral, with signal attenuation for species that have moved along z. By doing this experiment for a range of gradient strengths g, the peak integrals I will change, and the self-diffusion coefficients D can be calculated from

$$I = I_0 e^{-gbD}$$

where b contain parameters held constant and I_0 is the integral for $g = 0$. In Paper III, the cation, anion, and solvent diffusion could be measured individually since they each contain an exclusive NMR-active nucleus: ^{7}Li, ^{19}F in TFSI, which contains no H, and ^{1}H in the fluorine-free solvents.

3.3 Electrochemical methods

We will first look at the choice of reference electrode, relevant to many techniques, then turn to galvanostatic cycling, which is often one of the firsts tests of an elec-

trolyte, giving much information from a single experiment. Then follows measurement of ESWs using cyclic voltammetry (CV) and ion conductivity using electrochemical impedance spectroscopy (EIS).

3.3.1 Reference electrodes

The electrochemical tests are usually done in two or three-electrode cells; in the latter a separate reference electrode (R.E.) is used to avoid a shift in electrode potential when current is passed through the counter electrode (C.E.).[2] It also allows separate recording of the C.E. potential, which is useful both for full cell battery tests, and to avoid side reactions on the C.E. when running CV. In Paper I the electrolyte was not stable *vs.* Li metal, and as an alternative, LFP was used. To ensure a stable potential, the electrodes were partially de-lithiated in a separate cell. The recorded voltages are referenced against the R.E. and are transformed to use Li^+/Li as reference as $E_{\text{W.E. vs Li}} = E_{\text{LFP vs Li}} - E_{\text{W.E. measured}}$.

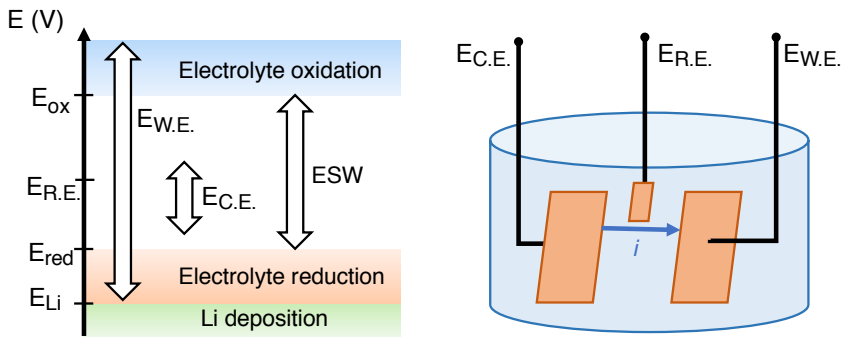

Figure 3.3. Left: potential diagram for a three electrode cell where $E_{W.E.}$ is swept across the voltage range. Right: a three electrode cell.

3.3.2 Battery cell cycling

The first practical test of how a battery electrolyte performs is typically *galvanostatic cycling*, *i.e.* using a constant current, of a two-electrode cell. This can give preliminary information on both electrode integrity and electrolyte stability, especially together with *post mortem* analysis.

Inspection of the voltage profiles not only reveals loss of capacity but also the magnitude and growth of cell polarization due to a range of factors such as electrolyte ionic conductivity and viscosity, SEI growth, electrolyte decomposition, or

[2]Here, C.E. is used for counter electrode, while CE is reserved for coulombic efficiency.

changes in electrode surface area. Differentiation of the capacity–voltage ($Q - V$) curves, *dQ/dV analysis* (Fig. 3.4) used in Paper I, results in peaks at the voltage of prominent reactions or plateaus of the electrode material, similar to CV (3.3.3). Differentiation using Savitzky–Golay filtering [67], which moves a locally fitted polynomial across the dataset, handles noisy measurement data much better than simple numeric differentiation.

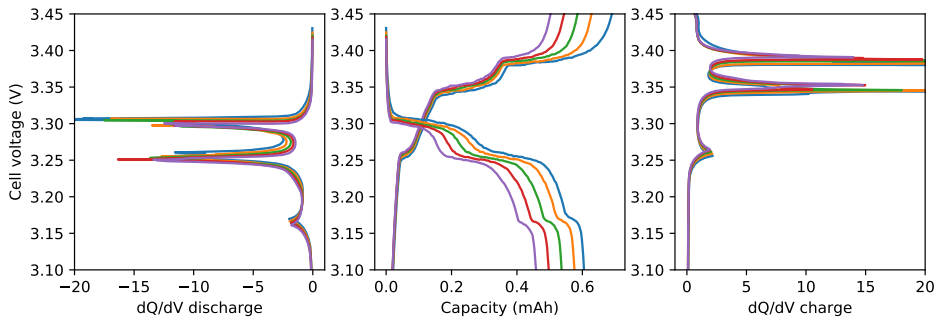

Figure 3.4. dQ/dV analysis of a graphite||LFP cell.

Coulombic efficiency (CE) is easily extracted as the ratio $Q_{\text{discharge}}/Q_{\text{charge}}$ when cycling full cells, but in a Li metal cell (Papers II & IV) the anode is typically not exhausted. This is why another method often is used to determine Li plating/stripping efficiency; Li is galvanostatically plated on *e.g.* Cu for a certain time (capacity) and then stripped until the Cu electrode is polarized to 1 V *vs.* Li^+/Li. More accurate measurements of Li metal CE are possible, *e.g.* using titration or through deposition of a Li buffer layer on the Cu substrate [68]. For comparisons across electrolytes, however, the method described with complete Li stripping is recommended [68] and less prone to fail.

To test the SEI stability, 120 h pauses at open circuit voltage (OCV) were used in the cycling scheme in Paper I. Pausing at high SOC tests the self-discharge [69, 70], which is either reversible or irreversible and observed as a capacity loss, implying that the electrode passivation was insufficient. A pause at low SOC probes the dissolution of the SEI through the need to re-passivate the electrode during the next charging step.

For the NMC cathodes in Paper IV, charge termination can be determined by a cut-off voltage, but the electrode is not strongly polarised at this stage, as in the case of LFP (Fig. 2.4b). In order to ensure a complete charge without destroying the electrode or electrolyte, a constant voltage is held at the end of the process, terminated when the current falls below a specified value.

3.3.3 Cyclic voltammetry (CV)

Whereas galvanostatic cycling applies a current and records the voltage, cyclic voltammetry (CV) sweeps the potential of the W.E. and records the resulting current. This reveals the potential at which electrode reactions occur. Also capacitance, reversibility of reactions, mass transfer limitation, kinetics and difference between surface-confined *vs.* solution reactions can be seen in a voltammogram.

To obtain a measure of the ESW, a common method is to only make a single *linear sweep* in each direction (ox/red) until the current dramatically increases. Instead of electrochemically active battery electrodes, blocking electrodes unable to sustain a Li^+ current are used, but in reduction tests, Li deposition can not be avoided. Since the useful ESW is determined not only by the electrolyte but also by the choice of electrodes, Cu and Al were selected in Paper I, since they are used as current collector for the battery electrodes. To see the effect of passivation or activation, multiple CV sweeps rather than a linear sweep were run.

When testing the reduction stability, only the reactions above Li plating were considered. The current was supported by oxidation and de-intercalation of Li from the LFP C.E. The potential of the C.E. was recorded to ensure to avoid electrolyte oxidation.[3] If the capacity of the C.E. is too low, *crosstalk* can occur: species other than Li oxidize at the C.E. to later get reduced at the W.E. When testing oxidation stability, LTO was used instead of LFP. The low ionic conductivity at high electrolyte salt concentrations result in cell resistance of 100's of ohms, which causes large *iR-drops* also between R.E. and W.E. (Fig. 3.3) which alters the recorded potential. This was compensated for by the instrument by first measuring the resistance with EIS (3.3.4).

3.3.4 Electrochemical impedance spectroscopy (EIS)

In electrochemical impedance spectroscopy (EIS), a sinusoidal voltage perturbation is applied to the cell, and the magnitude and phase of the current is recorded. The voltage must be small, typically < 10 mV, such that the current depends linearly on the voltage. The frequency f is stepped from *ca.* 0.1 Hz to 100 kHz or even 10 MHz in certain set-ups, giving the complex cell impedance $Z(f)$ as output. By fitting a circuit model to the data, parameters matching physical properties can be extracted, but the choice of equivalent circuit is not straightforward. A basic model that works reasonably for one electrode or a symmetric cell is the Randles circuit (Fig. 3.5): C_{DL} represents the double layer capacitance, R_S the electrolyte resistance, R_{CT} the charge transfer resistance for faradaic processes and W is the Warburg element representing diffusion to the electrode. Since different processes occur at different timescales, they can be separated from each other. In particular, R_S is given by $Z(f)$ at high f.

[3] This feature is absent from many instruments.

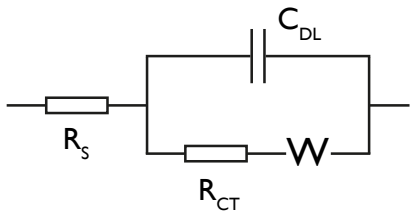

Figure 3.5. The Randles equivalent circuit model of an electrochemical cell.

For measuring electrolyte ionic conductivity σ in Papers I–III, a broadband dielectric spectrometer (BDS) connected to a programmable cryostat was used. The temperature was equilibrated at predetermined points before each measurement. Using blocking electrodes $R_{CT} = \infty$ and thus $R_S = Z(f)$ for high frequencies. The electrolyte ionic conductivity is then calculated from R_S, and note that the electrolyte ionic conductivity can not be measured using direct current and Ohm's law due to the electrode resistance R_{CT}.

Additional measurements were made with a bench-top conductivity meter with a dip-probe in Paper III in order to verify the EIS data. It operates similarly but automatically, and the dip-probe can be visually inspected to ensure complete electrode wetting, unlike the coin cells used in the BDS.

3.4 *Post mortem* analysis

After electrodes were cycled, cells were disassembled in a glovebox for visual inspection, and selected electrodes were investigated further. In this way the compatibility with separators and the cell layout can be tested. Indications are seen in *e.g.* discolouration of the separators, reactions with the current collectors, or deposits on electrodes.

3.4.1 X-ray photoelectron spectroscopy (XPS)

XPS probes the core electron binding energy E_b of atoms with a resolution < 0.3 eV. Since E_b is affected by interactions with the valence electrons, a shift indicating the chemical environment and oxidation state can be detected. Hence, XPS is not only for composition analysis in terms of atomic species, but can be used to distinguish between different compounds. The operating principle is to focus X-rays on the sample and detect the kinetic energy E_{kin} of the emitted electrons. The process is described by

$$h\nu = E_b + E_{\text{kin}} + \Phi$$

where $h\nu$ is the incident photon energy and Φ is the work function of the analyser. By increasing $h\nu$, E_{kin} will increase and, for a given mean free path, also the probe depth. The X-ray source of in-house instruments is limited to one or two energies, and typically the Al K_α source is used ($h\nu$ = 1486.4 eV), with a typical probe depth of a few nm [71]. To probe deeper or shallower, a tunable synchrotron X-ray source can be used. Sputtering with Ar ions can also reveal deeper layers, however with a risk for preferential sputtering of certain species.

XPS is one of the most important tools for investigation of electrode surfaces and the SEI in particular. Two important conditions for the experiment is a conductive sample and ultrahigh vacuum in the sample chamber which poses some restrictions on the sample. To study a cycled electrode, residual electrolyte must be removed since the vacuum removes all solvent. However, since washing may partially dissolve the SEI, multiple measurements with different degree of washing can be used.

To analyse the obtained spectra, references are needed that can sometimes be found in literature but may also have to be measured. An example is to compare cycled and pristine electrodes as in Paper I, or electrodes at different SOC. For the latter case, additional energy shifts arise from new electrostatic interactions.

Another complication that occurs for non-conductive surfaces is that the energy shifts because the probed atoms are not in electrical contact with the grounded sample holder, while charge builds up when electrons are photoemitted. It is common to calibrate towards ”adventious carbon”, using the C1s peak of adsorbed species from sample handling, and fixing them somewhere around 284–285 eV. This approach would be problematic in the case of Paper I, with large peaks from both graphite and organic SEI species, and has furthermore recently proven unreliable [72, 73]. In Paper I, the SEI was either conductive, thin or washed away enough to allow verification of spectral positions using the graphite peak, while checking other peaks for consistency.

3.4.2 Scanning electron microscopy (SEM)

SEM is a versatile technique based on scanning a beam of electrons across the sample rather than illuminating the whole sample with photons to form an image. The 0.2 µm diffraction limit of resolution is avoided and instead determined by the beam spot size and interaction volume, typically a few nm. Another benefit is the depth of field for simultaneous focus on objects near and far.

The SEM is well suited for morphology studies of Li metal plating (Paper II), easily spanning a magnification range from < 100 x for overview to > 100 000 x to reveal details on the surface of single Li features (Fig. 3.6). A low acceleration voltage and beam current (*e.g.* 3 kV, 100 pA) must be used to avoid melting Li when using high magnifications (a localized beam).

When imaging non-conductive samples such as polymeric separators, they must be coated with a thin metal film to avoid charging of the sample, which otherwise distorts the image by deflection of the scanning beam. The coating is made within minutes using a simple sputtering process. The charging can also tell something about SEI composition; if there is significant charging on plated Li metal, there is a substantial non-conductive cover, and if it furthermore melts easily under the beam, it is likely polymeric rather than inorganic.

An effective and thin SEI is difficult to observe using SEM, but on the graphite electrodes in Paper I, surface films were seen even with the naked eye, and thus some cycled graphite electrodes with different degree of solvent washing were studied. Electrodes from cells disassembled in the glovebox were transferred in a commercial transfer-box to the microscope.

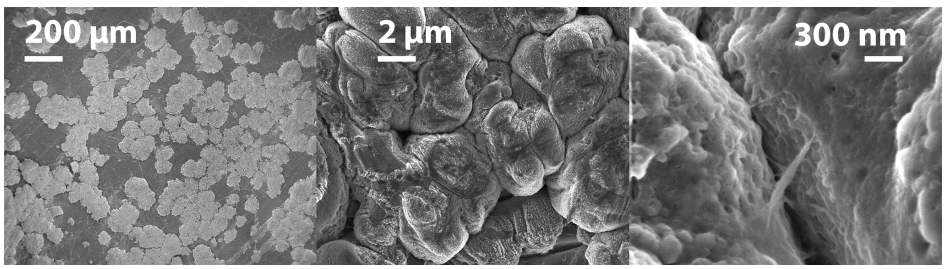

Figure 3.6. Li plated on Li foil studied in the SEM with different magnifications.

In order to investigate the Li morphology in Paper II, deposition was made on Cu substrates (Fig. 3.7), since tests using Li metal foil results in very inhomogeneous depositions that are difficult to reproduce. For cross-sections of Li metal, the electrodes can not be cut without smearing the Li. However, without any special tools, the Cu substrates can be torn apart with tweezers leaving a clean edge (Fig. 3.7).

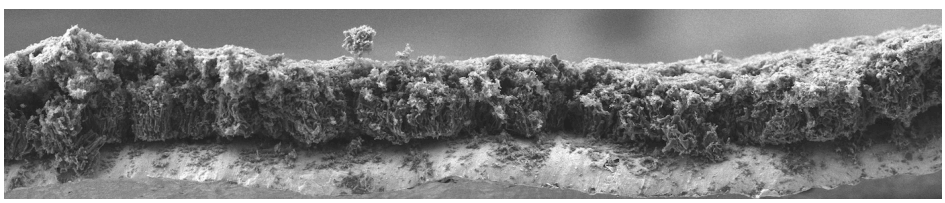

Figure 3.7. Cross-section of Li plated on Cu foil studied in the SEM.

4. Results and discussion

Here, the key results are presented and discussed. They are organized by topic rather than by paper and also include some additional results not found in any of the papers.

4.1 Re-assessing electrolytes based on inherently unstable components

Based on the reported electrochemical stability of LiTFSI–ACN HCEs [48], this was tested as a function of concentration *vs.* primarily graphite electrodes. In stark contrast to previous reports, galvanostatic cycling of the 1:1.9 LiTFSI:ACN HCE in a Li|| graphite cell resulted in fast capacity fading (Fig. 4.1a), mainly due to instability at the Li metal surface. The glass-fibre separator was attached to the Li electrode and full of electrolyte decomposition products and dendritic Li (Fig. 4.1b).

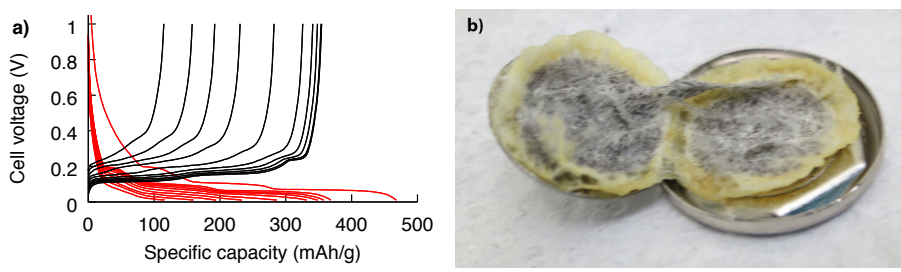

Figure 4.1. a) 10 cycles of a Li|1:1.9 LiTFSI:ACN|graphite cell, and b) the used glass-fibre separator.

This was the same electrolyte for which Yamada *et al.* reported stable cycling [48]. Only when the graphite loading was lowered from 1.9 mg/cm^2 to 0.3 mg/cm^2, a coating so thin that the current collector shines through (Fig. 4.2a), relatively stable cycling was achieved for both electrodes (Fig. 4.2b). With the thin coating, the areal current density is reduced when the C-rate is maintained, which is the best explanation for the increased stability, especially *vs.* the non-porous Li electrode. In contrast, storing Li foil in the electrolyte does not cause any noticeable electrolyte reduction.

By replacing the Li counter electrode with LFP, electrolytes of different concentration could be cycled *vs.* graphite electrodes of higher capacity. Limited by electrolyte decomposition at *ca.* 1.2 V *vs.* Li^+/Li, the graphite can not be fully lithiated

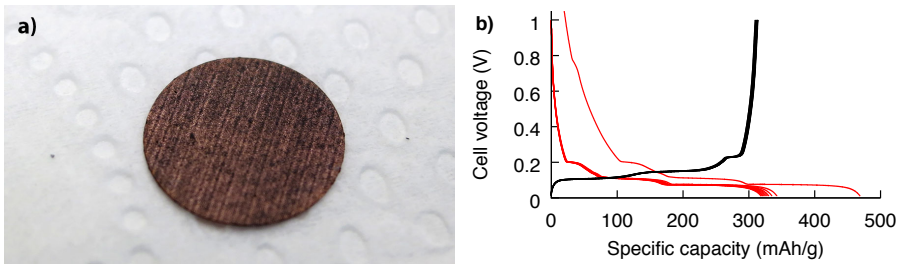

Figure 4.2. 0.3 mg/cm^2 graphite on Cu electrode, a) photo, and b) 10 cycles of a Li|1:1.9 LiTFSI:ACN|graphite cell.

using the lowest salt concentrations. For higher salt contents, the CE and the capacity retention improves until reaching the solubility limit (Fig. 4.3). The highest concentration, 1.1:67 LiTFSI:ACN, reaches a CE of 97% and a capacity retention of 78% which is still far from the reference cell using 1 M $LiPF_6$–EC:DEC. For the 1:1.9 LiTFSI:ACN electrolyte, the capacity loss is much higher than for the thin coating (Fig. 4.3b), again indicating the current density to be a dominating factor.

This strong dependence on current density suggests that a drop of salt concentration due to Li^+ depletion at the negative electrode during charging plays an important role. This leads to an increased concentration of free ACN just at the reducing electrode, a situation which is not mitigated by a low amount of free solvent in the bulk.

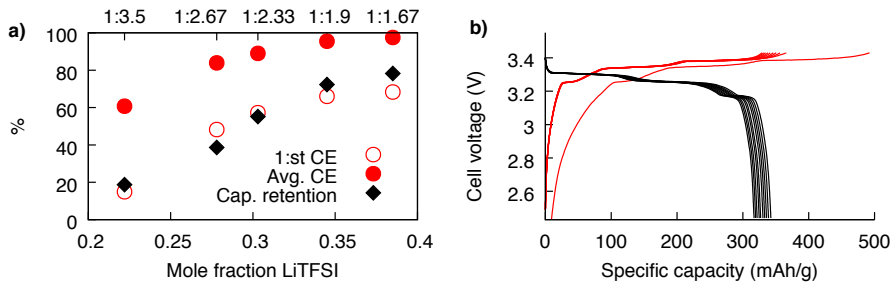

Figure 4.3. a) First cycle CE, average CE, and capacity retention of LiTFSI:ACN electrolytes in graphite||LFP cells, and b) 10 cycles of a graphite||LFP cell with 1.9 mg/cm^2 graphite.

Moving to the role of the SEI for cycling stability, SEI dissolution was probed using 120 h pauses at OCV during cycling. When the pauses were made at a high SOC, the cell self-discharged followed by a permanent capacity loss, indicating that an irreversible side-reaction occurred. In other words, there was degradation also without applied current. Pauses at a low SOC were not followed by a capacity loss, but a large overcapacity was required during the next charge; suggesting that the SEI had to reform because it had dissolved in the electrolyte.

To shine more light on the SEI and its concentration dependence, cycled graphite electrodes were analysed using XPS after a thorough wash in ACN. For the electrodes cycled in the less concentrated electrolytes, the signal of graphite was observed through the SEI to a larger extent, showing that the SEI was less dense or easily washed away. For the more concentrated electrolytes there was deposition of Li_3N, a higher quantity of insoluble fluoro-organics, and more oxidized S in the form of SO_4^{2-} or SO_2-units, all of which suggests that the SEI in the HCEs is mainly salt-derived. This has previously been interpreted as due to shifts in the HOMO levels of ACN and TFSI leading to preferential TFSI reduction [74]. Equally important is likely the much higher salt concentration and viscosity, which lead to a high presence of ions at the electrode, despite any current-induced concentration drop at the surface.

Finally, the electrochemical stability *vs.* Cu and Al electrodes was examined using CV (Fig. 4.4). The most important observation is that the potential for electrolyte reduction does not shift, showing that the ESW has not expanded towards lower potentials. Instead, the current is lowered, likely due to a mass transport limitation with less available solvent to reduce. The electrolyte reduction onset is *ca.* 1.2 V *vs.* Li^+/Li, equal to that of ACN reduction.

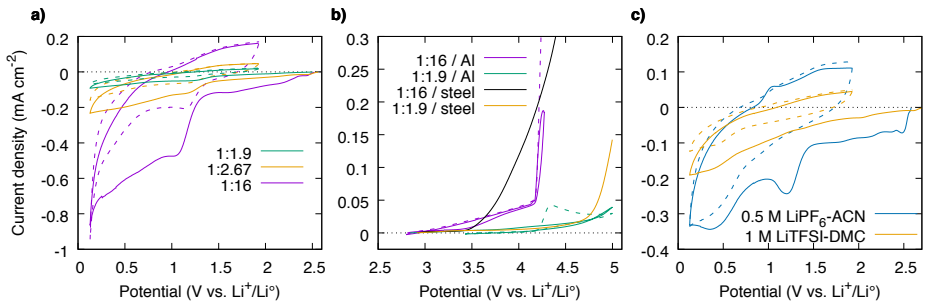

Figure 4.4. CVs of cycles 1 (solid) and 2 (dashed). a) Reduction test on Cu. b) Oxidation test on Al and steel, for 1:1.9 dashed shows cycle 100. c) Reduction test on Cu. Reproduced from Paper I with permission from Elsevier.

The oxidation stability *vs.* Al is increased from *ca.* 3 V to 4.2 V *vs.* Li^+/Li in 1:1.9 LiTFSI:ACN compared to the 1:16 electrolyte. The previously claimed stability up to 5 V *vs.* Li^+/Li [48] is not maintained over time on Al and oxidation stability on other electrodes is of marginal practical interest. After repeated cycles up to 5 V *vs.* Li^+/Li, an oxidation peak appears at 4.2 V *vs.* Li^+/Li, the same potential as where the current turns severe in 1:16 LiTFSI:ACN and can be attributed to Al dissolution.

In all, this electrolyte system shows some dramatic improvements when going to higher concentrations, but the instabilities observed nonetheless render this system uninteresting for practical purposes. It is also clear that the thermodynamic reduction potential was not altered and that the stabilization in this kind of HCE is highly dependent on the current density.

4.2 Application of inherently stable electrolytes *vs.* Li metal electrodes

With low hopes of defeating thermodynamics, the focus was turned to using it to our advantage and study electrolytes based on EC, a solvent known to be both electrochemically and physically stable. EC is able to form effective SEIs [26, 75] and has a boiling point of 243°C, but its melting point of *ca.* 36°C is a problem. With LiTFSI added in ratios 1:6 and 1:2 LiTFSI:EC, however, the liquid range is expanded down to *ca.* 0°C and −50°C, respectively [58].

In Paper II these two electrolytes were evaluated for application in LMBs targeting both energy density and safety. Additionally, two variations of the LiTFSI–EC electrolytes were tested: first 1:6 LiTFSI:PC, a substitution of EC with PC, and second 1 M LiTFSI–EC:DEC, as a "dilute" electrolyte (since dilute LiTFSI–EC mixtures are not liquid). The electrolyte 1 M LiTFSI + 0.2 M $LiNO_3$–DOL:DME, which is known from the field of Li-S batteries to offer stable Li metal cycling, was used as a reference.

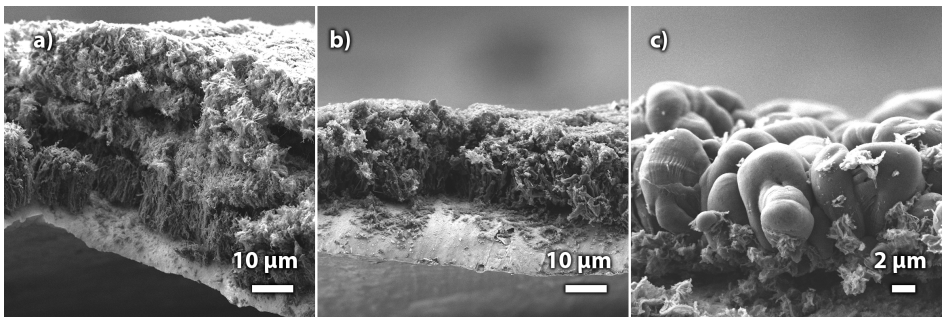

Figure 4.5. A Li film deposited on Cu after 4 prior plating/stripping cycles using electrolytes a) 1:6 LiTFSI:PC, b) 1:6 LiTFSI:EC, c) 1 M LiTFSI + 0.2 M $LiNO_3$–DOL:DME.

Due to continuous exposure to the electrolyte, the SEI that forms on the Li surface dictates the morphology of the deposited Li. In all carbonate-based electrolytes the Li film was made up of densely packed pillars, while in the DOL:DME-electrolyte, the Li was deposited as larger balls. This difference is mainly due to the presence of $LiNO_3$ in the latter electrolyte [76]. When the Li was repeatedly plated and stripped from the Cu substrate, there was an accumulation of "dead" material on the surface of the Li film, which was especially prominent for the 1:6 LiTFSI:PC and 1 M LiTFSI–EC:DEC electrolytes (Fig. 4.5a). This accumulation of layers correlate with a lower CE as well as a gradually increasing polarization in symmetric Li||Li cells using the same electrolytes. The lower CE likely lead to a thicker SEI on each deposited Li-strand, which during stripping leaves an empty "shell" that deposits on top of the electrode.

The CE shows that the DOL:DME electrolyte performs very well with a CE of 98.6%, followed by 1:6 LiTFSI:EC with a CE of 96.5% (Fig. 4.6a), while the PC-based electrolyte, as expected, has inferior stability. The dilute EC:DEC electrolyte also results in a much lower CE compared to the electrolyte based on only EC.

Additionally, $LiNO_3$ and DMC were tested as additives to 1:6 LiTFSI:EC in order to improve on the CE (Fig. 4.6b) (Paper IV). The solubility of $LiNO_3$ in 1:6 LiTFSI:EC is *ca.* 0.25 wt.% and is too low to make a significant difference, while DMC, just as DEC, has a negative effect on the CE. Since DMC was known to be a much better co-solvent than DEC for Li metal cycling [75], the large impact on efficiency was not expected.

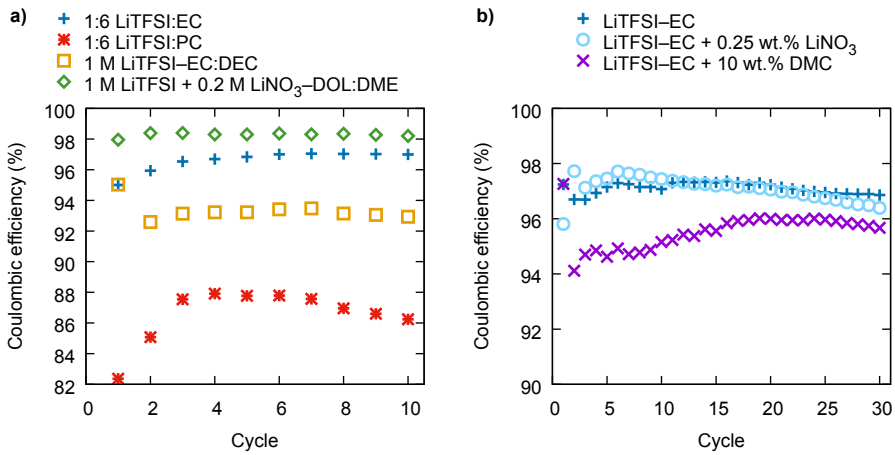

Figure 4.6. Coulombic efficiency of plating/stripping Li on a Cu substrate for a) different electrolytes, and b) 1:6 LiTFSI:EC with additives.

Apart from the high vapour pressure, a major drawback of the DOL:DME electrolyte is the limited oxidation stability of less than 3.6 V *vs.* Li^+/Li [77]. A test which simultaneously tests Li cycling efficiency and oxidation stability was made in a Cu||LFP cell. A limited electrolyte volume was used in order to reveal any inefficiencies as soon as possible; by not using a Li counter electrode, the available Li inventory is limited by the LFP capacity. Even with with the moderate voltage LFP electrodes, the 1:6 LiTFSI:EC electrolyte performed overall better than the 1 M LiTFSI + 0.2 M $LiNO_3$–DOL:DME (Fig. 4.7a).

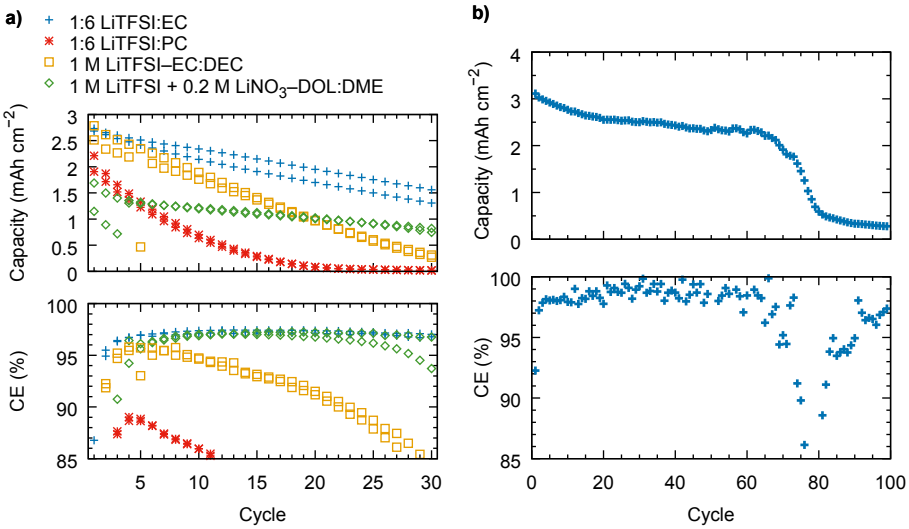

Figure 4.7. Cycling of a) Cu||LFP cells, and b) a Li||LFP cell using 1:6 LiTFSI:EC.

As a final proof of concept, a full LMB cell was assembled (Li||LFP) using the 1:6 LiTFSI:EC electrolyte (Fig. 4.7b). A 30 µm thin Li foil with only 1.8x overcapacity to the LFP capacity was used, in order to to achieve relevant energy densities [78]. Furthermore, the cell used an electrolyte loading of only 8.8 µl/cm^2 in a single 30 µm thin separator. Despite these harsh conditions, the cell cycled for *ca.* 70 cycles before failure. With further optimization of the cell, higher potential cathode materials, and additives to deal with possible Al current collector dissolution, all targeted in Paper IV, this approach may offer yet improved energy densities and cycle life.

4.3 Polymer separators for highly concentrated electrolytes

Due to the severe Li dendrite growth into the glass-fibre separator observed in Paper I and in the pilot tests for Paper II, a polymer membrane separator capable of blocking Li dendrites was highly desired. In addition, both Li metal cycling and *post mortem* analysis using SEM or XPS basically require another separator, but common poly(ethylene) or poly(propylene) separators are not wettable by the polar and viscous HCEs.

For Paper II, a 20 µm thin Solupor poly(ethylene) separator with high porosity was eventually wet by placing the electrolyte on both sides and letting the assembled cell rest at 50–70°C, while in Paper IV, separators based on the Solupor, but with hydrophilic coatings, showed significantly improved wetting ability. In LIB rate tests, however, the uncoated separator performed better, which was ascribed to the higher

permeability; thinner, less turbid, and larger pores. This shows a way forward; thinner and hydrophilic separators should allow for both fast cell manufacturing and high performance cells.

4.4 Ionic transport in highly concentrated electrolytes

In Paper III the fundamentals of ionic transport in HCEs were investigated using electrolytes based on 3 solvents for the LiTFSI salt in 3 salt concentrations. Both physico-chemical data collection as well as practical cell tests were performed to connect the fundamental properties to LIB rate capabilities.

First, the viscosities were low and similar for the more dilute electrolytes, with each higher salt concentration resulting in roughly an order of magnitude higher viscosity (Fig. 4.8a).

If the salt is dissociated, the ionic conductivity should be inversely related to the viscosity, which is true for the PC-based electrolytes. For all the MTBE-based electrolytes, the ionic conductivity is much lower (Fig. 4.8b), suggesting that ion-pairing occurs, unsurprising given the low solvent permittivity.

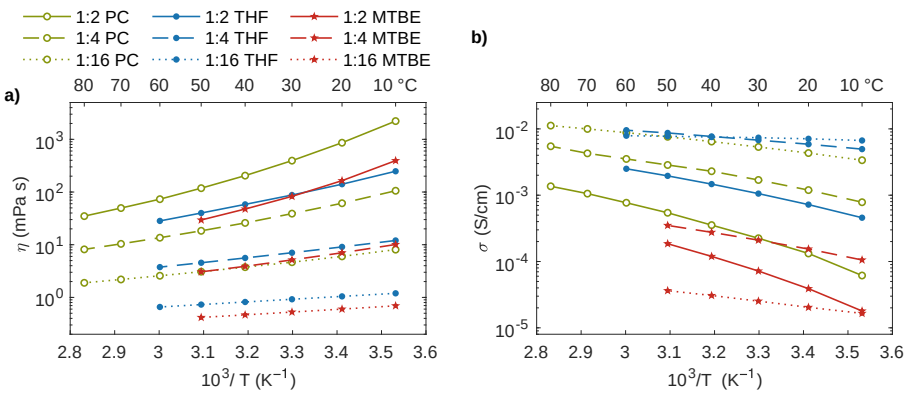

Figure 4.8. a) electrolyte viscosities, and b) electrolyte ionic conductivities

Having a similar viscosity and only slightly higher polarity, the THF-based electrolytes perform much better. In contrast, all the HCEs show very high viscosities and very low ionic conductivities, despite their higher ion density. In a Walden plot (Fig. 4.9a) the distance from the diagonal line shows ionicity, which increases with concentration for both MTBE and THF based electrolytes with clear ion-pairing for the MTBE-based electrolytes and dilute 1:16 THF. While the high salt concentrations necessarily lead to ionic association, from an ionic transport perspective the ions appear more free.

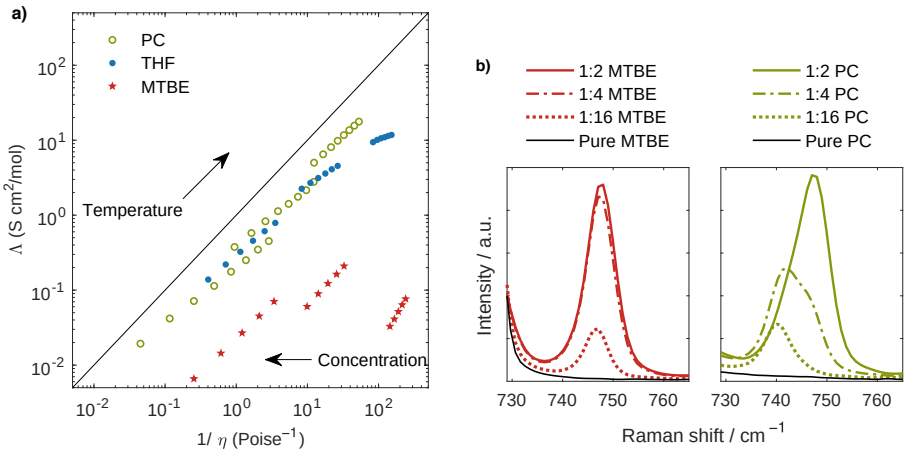

Figure 4.9. a) Walden plot of molar conductivity *vs.* fluidity, and b) Raman spectra for the region 729–765 cm^{-1} showing TFSI breathing in electrolytes based on MTBE and PC.

Ion aggregation in the MTBE-based electrolytes was verified by Raman spectroscopy, where the TFSI anion was observed as Li-coordinated even at the lowest concentration (Fig. 4.9b). The PC-based electrolytes in contrast show almost exclusively free TFSI for the dilute electrolyte, Li-coordinated TFSI for the 1:2 electrolyte, and an intermediate picture for the 1:4 electrolyte.

The diffusivity measurements of the electrolytes using PFG-NMR again showed aggregation in the dilute THF and MTBE electrolytes, which seems to increase with temperature. The ionicities derived from the diffusivities using the Nernst-Einstein equation overall agree with the conclusions above. Transport numbers were also derived, which as a consequence of ion-pairing and the use of self-diffusion coefficients without external electric fields, all were close to 0.5.

The rate capabilities were tested using all of the nine model electrolytes with 1 M $LiPF_6$–EC:DEC as a reference. For comparison, the 1:6 LiTFSI:EC electrolyte from Paper II was tested in the same way (Fig. 4.10).

The electrolyte property with most impact on the rate capability is the electrolyte ionic conductivity, with all HCEs and all MTBE-based electrolytes showing much lower discharge capacities. Between the three electrolytes with the highest, roughly equal ionic conductivities, 1:16 PC, 1:16 THF and 1:4 THF, the capacities are similar. The energy efficiency is higher, however, for 1:16 THF, as can be seen as a less sloping discharge voltage at high rates (Fig. 4.11). This is likely due to the lower viscosity.

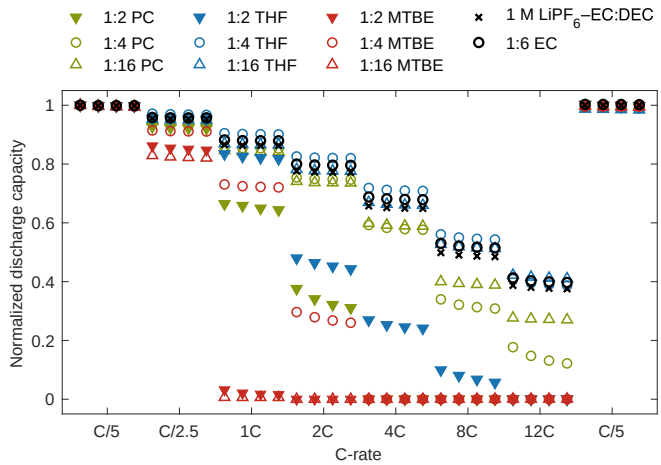

Figure 4.10. Rate test of the different electrolytes in LTO||LFP cells

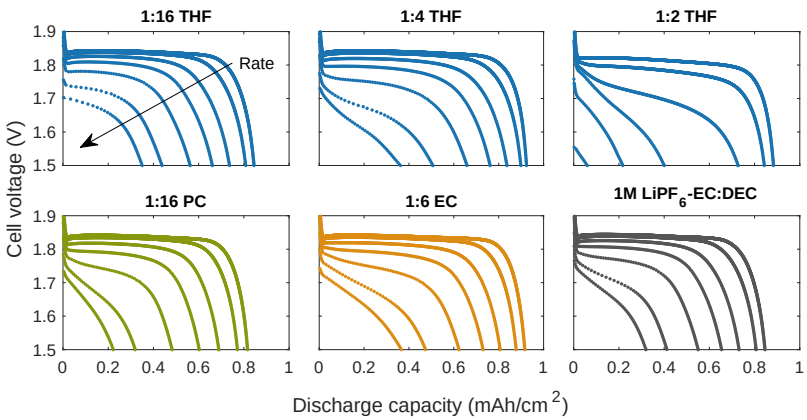

Figure 4.11. Selected discharge voltage profiles for rates C/5, C/2.5, 1C, 2C, 4C, 8C and 12C tested at 30°C with 1C=1 mA/cm^2.

4.5 Using LiTFSI-EC based electrolytes *vs.* high voltage cathodes

The LiTFSI–EC electrolyte from Paper II, 1:6 LiTFSI:EC, has the potential to offer increased safety also in LIBs. Since the limiting electrode in the LMBs was the Li metal anode, moving to graphite anodes could take the electrolyte closer to a viable product. As the LFP cathode has a relatively low potential and hence limited energy density, the cathode was replaced by NMC622 using a charging cut-off potential of 4.3 V *vs.* Li^+/Li. This leads to a challenge to avoid dissolution of the Al current collector in the LiTFSI-based electrolyte. To tackle the Al instability, $LiPF_6$ and $LiBF_4$ were added to the LiTFSI–EC electrolyte to get sacrificially decomposed and form a passivating film on the Al.

First, using chronoamperometry (Fig. 4.12a), an effective passivation up to 4.25 V *vs.* Li^+/Li using either additive was shown, while the stock electrolyte had significant currents already at 3.75 V *vs.* Li^+/Li. Thereafter, cycling of graphite||NMC622 cells showed early cell failure when using the electrolyte without additives, while stable cell cycling was achieved using the $LiPF_6$ additive, as for the reference electrolyte (Fig. 4.12b). The cell with the $LiBF_4$ additive suffered from continuous capacity fading and lower CE, possibly due to the presence of water which is very difficult to remove from BF_4 salts.

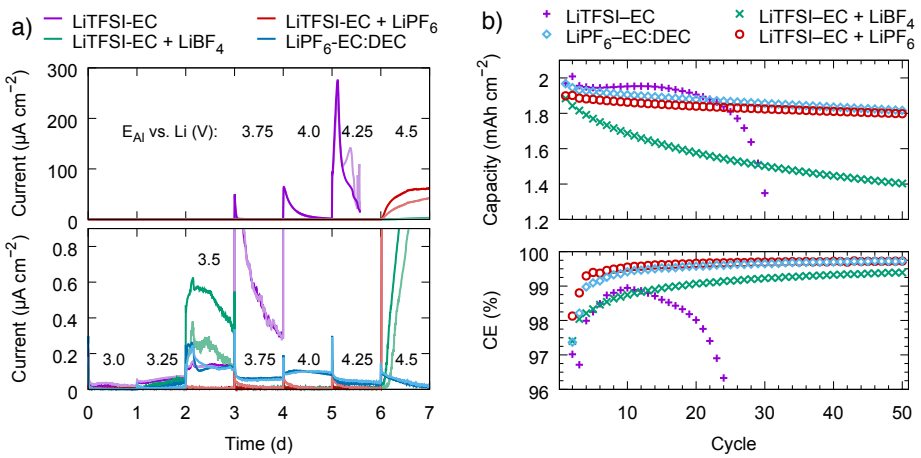

Figure 4.12. a) Chronoamperometry in Li||Al cells with cell voltages as indicated inside, and b) galvanostatic cycling at C/5 in graphite||NMC622 cells between 2.8 and 4.2 V.

In contrast to the cycling in full cells, when the electrolytes were compared in Li||NMC622 half-cells charged to 4.3 V *vs.* Li^+/Li, the cell with the $LiPF_6$ additive failed after two cycles with a reaction at *ca.* 3.7 V *vs.* Li^+/Li, characteristic of Al dissolution (Fig. 4.13).

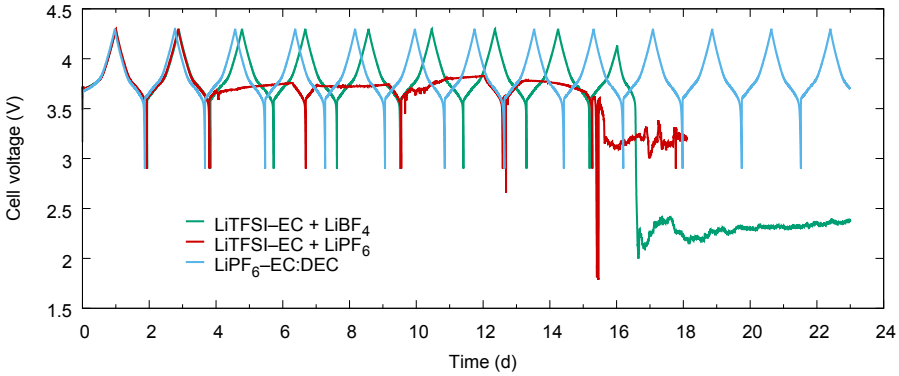

Figure 4.13. Li||NMC622 cells cycled at C/20.

The discrepancy when comparing to the full cell above could be due to a slightly higher electrode potential or instability on the Li counter electrode similar to the one in Paper I. The much sharper rise in current for LiTFSI–EC + $LiPF_6$ compared to LiTFSI–EC + $LiBF_4$ suggest that the former is more sensitive to high potentials. A higher concentration of additive salts can help to increase the margins towards Al dissolution, but crystallization of the electrolyte is a problem. This can likely be solved by adding PC as a co-solvent, which overall suggests that the LiTFSI–EC + $LiPF_6$ electrolyte is promising as a liquid electrolyte for safer LIBs.

5. Concluding remarks and outlook

To be able to take a highly unstable electrolyte and stabilize it by increasing the salt concentration may sound impressive, but it appears as if some drawbacks generally will persist. In particular the presence of free solvent with applied current is difficult to avoid in this approach to HCEs. Even moving to more stable components such as when using flame retardants as solvent [79], the electrochemical stability is again derived from the high salt concentration and unlikely to provide significant LIB cycle life.

In contrast, an electrolyte based on effectively passivating components such as EC and using appropriate additives is a more realistic way forward. The requirements on the electrochemical stability is ultimately to compete with the current LIB electrolytes which already are very good [80]. Creating an eutectic liquid electrolyte from solid components, such as the LiTFSI–EC electrolyte or deep eutectic solvents [81, 82] is a fundamentally different approach, where instead of fighting thermodynamics, we can use it to our advantage. Indeed, the LiTFSI–EC electrolyte has adequate cycling performance using Li metal anodes and is furthermore able to wet a thin polymer separator which proves applicability of the concept.

The investigations of ion transport and rate tests show no beneficial properties of the HCEs. However, there are reports of significantly increased cation transference numbers [56] and improved rate capability [44] for some HCEs, why further investigation of the mechanisms and generality of these phenomena are desired. For a fundamental understanding and to support modeling, more advanced measurements of transference numbers of HCEs are required. One way is to use electrophoretic NMR, in which an applied electric field drives the ions which better emulate the transport in a battery cell. For use in commercial LIBs, locally concentrated or diluted HCEs with lower cost and viscosity are perhaps more promising [83–85]. Regardless of the detailed solution structure, research in this area can lead to successful combinations of previously untried solvent combinations. There is, however, still hope for the HCE — the LiTFSI–EC electrolyte surprisingly showed a rate capability on par with 1 M $LiPF_6$–EC:DEC which again suggests that this HCE is practically useful.

Using HCEs can improve the battery cell safety through a lowered vapour pressure given that the system is electrochemically stable. Other means of improving safety such as flame retardants and polymer electrolytes have significant drawbacks

in terms of electrochemical stability and ionic conductivity, respectively. Using an electrolyte based on LiTFSI–EC can be favourable; it is not only non-volatile, but a decreased amount of $LiPF_6$ should improve stability at higher temperatures. High temperature cycling together with full cell safety tests are therefore the next steps for this electrolyte to overcome.

To summarize, the combination of an inherently unstable electrolyte, low ionic conductivity, higher density and high cost may not offer much for the next generation of LIBs, but are interesting from a physical chemistry perspective, and with water-based concepts and cheaper salts HCEs could still be practically relevant. The non-volatile LiTFSI–EC electrolytes are surprisingly stable *vs.* both Li metal and NMC622 electrodes, and could possibly be used where safety or temperature requirements outweigh the increased costs.

Some concrete ways forward are

- For a better understanding of transport in HCEs, measure transference numbers using electrophoretic NMR, including also glyme and sulfolane based electrolytes for which high rate capabilities have been reported.

- Test LIBs using LiTFSI–EC *vs.* NMC cathodes at elevated temperatures and longer times including *post mortem* analysis of Al current collectors.

- Investigate further electrolytes based on inherently stable solvents, including EC–PC mixtures to further decrease the melting point and allow higher additive loadings.

- Perform safety tests of HCEs, LiTFSI–EC in particular, by short circuiting high energy prototype cells in order to assess any real safety improvements.

6. Sammanfattning på svenska (Summary in Swedish)

Elektrolyten är en fundamental del av ett litiumbatteri som starkt påverkar livslängden och säkerheten. Den måste utstå svåra förhållanden, inte minst vid gränsytan mot elektroderna. Dagens kommersiella elektrolyter är baserade på 1 M $LiPF_6$ i en blandning av organiska lösningsmedel. De balanserar kraven på elektrokemisk stabilitet och jonledningsförmåga, men de är lättflyktiga och bryts ned när de används vid temperaturer över ca. 70°C. Saltet skulle kunna bytas ut mot t.ex. LiTFSI, vilket skulle öka värmetåligheten avsevärt, men istället uppstår problem med korrosion på den strömuppsamlare av aluminium som används för katoden.

Genom att byta ut grafitanoden i ett Li-jonbatteri mot en folie av litiummetall kan man öka energitätheten, men då litium pläteras bildas ständigt nya Li-ytor som kan reagera med elektrolyten. Detta leder till en låg *coulombisk effektivitet* genom nedbrytning av både Li och elektrolyt.

En fördel med LiTFSI är att det går att lösa i höga saltkoncentrationer och bilda *högkoncentrerade elektrolyter* vilka har lagts fram som en möjlig lösning på många av de problem som plågar denna och nästa generations batterier. Dessa elektrolyter har en annorlunda lösningsstruktur — alla lösningsmedelsmolekyler koordinerar till katjoner – vilket leder till att de blir mindre lättflyktiga, får en ökad täthet av laddningsbärare och en ökad elektrokemisk stabilitet. Samtidigt får de en högre viskositet och lägre jonledningsförmåga. Här har olika angreppssätt för högkoncentrerade elektrolyter baserade på LiTFSI utvärderats och fundamentala transportegenskaper mätts.

I artikel I har acetonitril som har en starkt begränsad elektrokemisk stabilitet och en hög volatilitet, blandats med LiTFSI resulterande i en uppsättning av elektrolyter med varierande saltkoncentration. Dessa har testats i Li-jonbatterier och i synnerhet den passiverade ytan på grafitelektroderna har undersökts med både röntgenfotoelektronspektroskopi (XPS) och elektrokemiska metoder. Den höga saltkoncentrationen sänker volatiliteten och ger en markant förbättring av den elektrokemiska stabiliteten, men de inneboende bristerna hos elektrolyten kan inte kompenseras fullständigt. I synnerhet syns ett starkt beroende på strömtätheten på elektroderna, där en väldigt låg ström kan hanteras, men så fort man närmar sig strömmar relevanta för tillämp-

ningar reduceras elektrolytens lösningsmedel. Detta skapar tvivel på hur väl detta kan fungera i en kommersiell cell.

I artikel II används ett annat angreppssätt, där en hög saltkoncentration nyttjats för att sänka smältpunkten hos en elektrolyt baserad på etylenkarbonat (EC), som är fast vid rumstemperatur och annars inte kan används som enda lösningsmedel. Etylenkarbonat har ett väldigt lågt ångtryck och en hög kokpunkt vilket leder till en inneboende hög säkerhet och möjlighet att använda batterierna vid högre temperaturer. Elektrolyten EC–LiTFSI uppvisar lovande prestanda vid cykling av litiummetall och till skillnad från en referenselektrolyt är den samtidigt kompatibel med katodmaterial och ett litium-metallbatteri kunde cyklas ca. 70 gånger. Dessutom väter elektrolyten en 20 µm tunn separator, vilket gör elektrolyten tillämpbar i fullskaliga celler.

I artikel III har jontransporten i högkoncentrerade elektrolyter undersökts för att se hur egenskaper såsom konduktivitet, viskositet och jonicitet (jondissociation) avspeglas i Li-jonbatteriers maximala laddningshastighet. Det framstår som att joniciteten ur transporthänseende ökar med en högre saltkoncentration, även om jonerna är i närmare kontakt. Däremot har de högkoncentrerade elektrolyterna överlag inte några positiva effekter på cellprestanda eller transport, något som skiljer från många tidigare rapporter.

EC–LiTFSI-elektrolyterna från artikel II testades i artikel IV i Li-jonbatterier med NMC-katoder för att åstadkomma celler med högre spänning. Tillsatser av andra Li-salt passiverade strömuppsamlaren av aluminium och resulterade i en jämförbar prestanda med en kommersiell elektrolyt både i termer av urladdningshastighet och kapacitetsbevarande. För denna elektrolyt kvarstår arbete med att bevisa en förbättrad livslängd av batteriet över tid och säkerhetstester av uppskalade celler. Sammantaget har denna elektrolyt visat ett förvånansvärt lovande resultat utifrån vad som kunde förväntas från dess fysikal-kemiska egenskaper.

7. Acknowledgements

First of all, I would like to thank my main supervisors Patrik and Kristina for making this possible. For setting the bar high and forcing me to work independently, and for hosting me in two different but equally creative environments. Reza, your suggestions on experiments have been very helpful. Daniel, you have been around and seen pragmatic solutions to all kinds of problems. Aleksandar, thanks for approving my expenses, and also for advice on my work.

I am grateful for the good collaboration with my additional co-authors: Andoria, my SEM partner in crime, Diana who was immensely helpful with NMR expertise, and Matthew L, not only for the suggestions on Paper II, but also plenty of discussions and good fun. Others who were directly helpful with experiments or manuscript/thesis feedback and deserve mention are: Adriana, Burak, Carmen, Christofer, Dennis, Laura, Pierre-Alexandre, Piotr, Rassmus, Roza.

I also would like to thank...

...all my current and former colleagues, at Uppsala University and at Chalmers, for many work-related discussions, and lots of fun after work.

...the administrators Eva Larsson and Anna Lindqvist.

...Ezio and Henrik, who kept the labs running and always were open for discussion.

...everyone who asked me questions or gave me feedback on oral presentations.

...Jonathan, Torbjörn and Lars for teaching and course development opportunities.

...Henrik, my first scientific supervisor, long before this project.

For funding me, I acknowledge Alistore-European Research Institute and the Swedish Energy Agency, the latter through ”Batterifondsprogrammet” #39042-1, using money previously collected from battery producers. Additionally for paying my trips to England and South Africa, thanks to Anna Maria Lundins stipendiefond at Smålands nation, Liljewalchs, ÅForsk and Nils Pihlblads stipendiefond.

Lastly, thanks to all support from my girlfriend Lova, my family and all my friends.

Bibliography

[1] Nishi Yoshio, "The development of lithium ion secondary batteries", *The Chemical Record*, vol. 1, no. 5, pp. 406–413, Sep. 13, 2001. DOI: 10.1002/tcr.1024.

[2] W. Li, E. M. Erickson, and A. Manthiram, "High-nickel layered oxide cathodes for lithium-based automotive batteries", *Nat. Energy*, vol. 5, no. 1, pp. 26–34, Jan. 2020. DOI: 10.1038/s41560-019-0513-0.

[3] M. M. Waldrop, "The chips are down for Moore's law", *Nat. News*, vol. 530, no. 7589, p. 144, Feb. 11, 2016. DOI: 10.1038/530144a.

[4] *2019 OPEC World Oil Outlook*. Vienna: OPEC Secretariat, Oct. 2019. [Online]. Available: http://www.opec.org (visited on 04/13/2018).

[5] "Global EV Outlook 2019", International Energy Agency, 2019.

[6] E. S. Takeuchi and M. M. Doeff, "An Argument for Basic Battery Science: Each Time an Application Demands a New Battery Chemistry To Achieve Previously Unrealized Functionality, a New Fundamental Understanding Is Required", *Acc. Chem. Res.*, vol. 51, no. 3, pp. 573–574, Mar. 20, 2018. DOI: 10.1021/acs.accounts.8b00078.

[7] K. Xu, "Electrolytes and Interphases in Li-Ion Batteries and Beyond", *Chem. Rev.*, vol. 114, no. 23, pp. 11 503–11 618, Dec. 10, 2014. DOI: 10.1021/cr500003w.

[8] E. Peled and S. Menkin, "Review—SEI: Past, Present and Future", *J. Electrochem. Soc.*, vol. 164, no. 7, A1703–A1719, Jan. 1, 2017. DOI: 10.1149/2.1441707jes.

[9] M. R. Palacín and A. de Guibert, "Why do batteries fail?", *Science*, vol. 351, no. 6273, p. 1 253 292, Feb. 5, 2016. DOI: 10.1126/science.1253292. pmid: 26912708.

[10] Y. Yamada and A. Yamada, "Review—Superconcentrated Electrolytes for Lithium Batteries", *JES*, vol. 162, no. 14, A2406–A2423, Jan. 1, 2015. DOI: 10.1149/2.0041514jes.

[11] *Oxford Dictionary of English*. Oxford University Press, 2016.

[12] R. Zhao, J. Liu, and J. Gu, "Simulation and experimental study on lithium ion battery short circuit", *Applied Energy*, vol. 173, pp. 29–39, Jul. 1, 2016. DOI: 10.1016/j.apenergy.2016.04.016.

[13] T. Ohzuku, Y. Iwakoshi, and K. Sawai, "Formation of Lithium-Graphite Intercalation Compounds in Nonaqueous Electrolytes and Their Application as a Negative Electrode for a Lithium Ion (Shuttlecock) Cell", *J. Electrochem. Soc.*, vol. 140, no. 9, pp. 2490–2498, Jan. 9, 1993. DOI: 10.1149/1.2220849.

[14] H. Wu and Y. Cui, "Designing nanostructured Si anodes for high energy lithium ion batteries", *Nano Today*, vol. 7, no. 5, pp. 414–429, Oct. 1, 2012. DOI: 10.1016/j.nantod.2012.08.004.

[15] X. Li, A. M. Colclasure, D. P. Finegan, D. Ren, Y. Shi, X. Feng, L. Cao, Y. Yang, and K. Smith, “Degradation mechanisms of high capacity 18650 cells containing Si-graphite anode and nickel-rich NMC cathode”, *Electrochimica Acta*, vol. 297, pp. 1109–1120, Feb. 20, 2019. DOI: 10.1016/j.electacta.2018.11.194.

[16] D. Lin, Y. Liu, and Y. Cui, “Reviving the lithium metal anode for high-energy batteries”, *Nat Nano*, vol. 12, no. 3, pp. 194–206, Mar. 2017. DOI: 10.1038/nnano.2017.16.

[17] J.-G. Zhang, W. Xu, and W. A. Henderson, “High Coulombic Efficiency of Lithium Plating/Stripping and Lithium Dendrite Prevention”, in *Lithium Metal Anodes and Rechargeable Lithium Metal Batteries*, ser. Springer Series in Materials Science 249, Springer International Publishing, 2017, pp. 45–152. [Online]. Available: http://link.springer.com/chapter/10.1007/978-3-319-44054-5_3 (visited on 02/27/2017).

[18] X. Sun, P. V. Radovanovic, and B. Cui, “Advances in spinel Li4Ti5O12 anode materials for lithium-ion batteries”, *New J. Chem.*, vol. 39, no. 1, pp. 38–63, Dec. 17, 2014. DOI: 10.1039/C4NJ01390E.

[19] G. Zubi, R. Dufo-López, M. Carvalho, and G. Pasaoglu, “The lithium-ion battery: State of the art and future perspectives”, *Renewable and Sustainable Energy Reviews*, vol. 89, pp. 292–308, Jun. 2018. DOI: 10.1016/j.rser.2018.03.002.

[20] R. Schmuch, R. Wagner, G. Hörpel, T. Placke, and M. Winter, “Performance and cost of materials for lithium-based rechargeable automotive batteries”, *Nat. Energy*, vol. 3, no. 4, pp. 267–278, Apr. 2018. DOI: 10.1038/s41560-018-0107-2.

[21] T. C. Frankel, “Cobalt mining for lithium ion batteries has a high human cost - Washington Post”, *The Washington Post*, Sep. 30, 2016. [Online]. Available: https://www.washingtonpost.com/graphics/business/batteries/congo-cobalt-mining-for-lithium-ion-battery/ (visited on 05/15/2018).

[22] K. Xu, “Nonaqueous Liquid Electrolytes for Lithium-Based Rechargeable Batteries”, *Chem. Rev.*, vol. 104, no. 10, pp. 4303–4418, Oct. 1, 2004. DOI: 10.1021/cr030203g.

[23] R. Petibon, J. Xia, L. Ma, M. K. G. Bauer, K. J. Nelson, and J. R. Dahn, “Electrolyte System for High Voltage Li-Ion Cells”, *J. Electrochem. Soc.*, vol. 163, no. 13, A2571–A2578, Jan. 1, 2016. DOI: 10.1149/2.0321613jes.

[24] E. Peled, “The Electrochemical Behavior of Alkali and Alkaline Earth Metals in Nonaqueous Battery Systems—The Solid Electrolyte Interphase Model”, *J. Electrochem. Soc.*, vol. 126, no. 12, pp. 2047–2051, Jan. 12, 1979. DOI: 10.1149/1.2128859.

[25] P. Verma, P. Maire, and P. Novák, “A review of the features and analyses of the solid electrolyte interphase in Li-ion batteries”, *Electrochimica Acta*, vol. 55, no. 22, pp. 6332–6341, Sep. 1, 2010. DOI: 10.1016/j.electacta.2010.05.072.

[26] L. Xing, X. Zheng, M. Schroeder, J. Alvarado, A. von Wald Cresce, K. Xu, Q. Li, and W. Li, “Deciphering the Ethylene Carbonate–Propylene Carbonate Mystery in Li-Ion Batteries”, *Acc. Chem. Res.*, vol. 51, no. 2, pp. 282–289, Feb. 20, 2018. DOI: 10.1021/acs.accounts.7b00474.

[27] B. Aktekin, R. Younesi, W. Zipprich, C. Tengstedt, D. Brandell, and K. Edström, “The Effect of the Fluoroethylene Carbonate Additive in LiNi0.5Mn1.5O4 - Li4Ti5O12 Lithium-Ion Cells”, *J. Electrochem. Soc.*, vol. 164, no. 4, A942, Mar. 8, 2017. DOI: 10.1149/2.0231706jes.

[28] S. E. Sloop, J. K. Pugh, S. Wang, J. B. Kerr, and K. Kinoshita, "Chemical Reactivity of PF_5 and $LiPF_6$ in Ethylene Carbonate/Dimethyl Carbonate Solutions", *Electrochem. Solid-State Lett.*, vol. 4, no. 4, A42–A44, Jan. 4, 2001. DOI: 10.1149/1.1353158.

[29] M. Stich, M. Göttlinger, M. Kurniawan, U. Schmidt, and A. Bund, "Hydrolysis of LiPF6 in Carbonate-Based Electrolytes for Lithium-Ion Batteries and in Aqueous Media", *J. Phys. Chem. C*, vol. 122, no. 16, pp. 8836–8842, Apr. 26, 2018. DOI: 10.1021/acs.jpcc.8b02080.

[30] R. Younesi, G. M. Veith, P. Johansson, K. Edström, and T. Vegge, "Lithium salts for advanced lithium batteries: Li–metal, Li–O2, and Li–S", *Energy Environ. Sci.*, vol. 8, no. 7, pp. 1905–1922, Jul. 3, 2015. DOI: 10.1039/C5EE01215E.

[31] D. M. Seo, O. Borodin, S.-D. Han, P. D. Boyle, and W. A. Henderson, "Electrolyte Solvation and Ionic Association II. Acetonitrile-Lithium Salt Mixtures: Highly Dissociated Salts", *J. Electrochem. Soc.*, vol. 159, no. 9, A1489–A1500, Jan. 1, 2012. DOI: 10.1149/2.035209jes.

[32] S.-D. Han, O. Borodin, D. M. Seo, Z.-B. Zhou, and W. A. Henderson, "Electrolyte Solvation and Ionic Association V. Acetonitrile-Lithium Bis(fluorosulfonyl)imide (LiFSI) Mixtures", *J. Electrochem. Soc.*, vol. 161, no. 14, A2042–A2053, Jan. 1, 2014. DOI: 10.1149/2.0101414jes.

[33] C. G. Barlowz, "Reaction of Water with Hexafluorophosphates and with Li Bis(perfluoroethylsulfonyl)imide Salt", *Electrochem. Solid-State Lett.*, vol. 2, no. 8, pp. 362–364, Jan. 8, 1999. DOI: 10.1149/1.1390838.

[34] M. Kerner, N. Plylahan, J. Scheers, and P. Johansson, "Thermal stability and decomposition of lithium bis(fluorosulfonyl)imide (LiFSI) salts", *RSC Adv.*, vol. 6, no. 28, pp. 23 327–23 334, 2016. DOI: 10.1039/C5RA25048J.

[35] D. Di Censo, I. Exnar, and M. Graetzel, "Non-corrosive electrolyte compositions containing perfluoroalkylsulfonyl imides for high power Li-ion batteries", *Electrochemistry Communications*, vol. 7, no. 10, pp. 1000–1006, Oct. 2005. DOI: 10.1016/j.elecom.2005.07.005.

[36] H.-B. Han, S.-S. Zhou, D.-J. Zhang, S.-W. Feng, L.-F. Li, K. Liu, W.-F. Feng, J. Nie, H. Li, X.-J. Huang, M. Armand, and Z.-B. Zhou, "Lithium bis(fluorosulfonyl)imide (LiFSI) as conducting salt for nonaqueous liquid electrolytes for lithium-ion batteries: Physicochemical and electrochemical properties", *Journal of Power Sources*, vol. 196, no. 7, pp. 3623–3632, Apr. 1, 2011. DOI: 10.1016/j.jpowsour.2010.12.040.

[37] V. Sharova, A. Moretti, T. Diemant, A. Varzi, R. J. Behm, and S. Passerini, "Comparative study of imide-based Li salts as electrolyte additives for Li-ion batteries", *Journal of Power Sources*, vol. 375, pp. 43–52, Jan. 31, 2018. DOI: 10.1016/j.jpowsour.2017.11.045.

[38] C. Zhong, Y. Deng, W. Hu, J. Qiao, L. Zhang, and J. Zhang, "A review of electrolyte materials and compositions for electrochemical supercapacitors", *Chem. Soc. Rev.*, vol. 44, no. 21, pp. 7484–7539, 2015. DOI: 10.1039/C5CS00303B.

[39] M. Hagen, D. Hanselmann, K. Ahlbrecht, R. Maça, D. Gerber, and J. Tübke, "Lithium–Sulfur Cells: The Gap between the State-of-the-Art and the Requirements for High Energy Battery Cells", *Adv. Energy Mater.*, vol. 5, no. 16, p. 1 401 986, Aug. 1, 2015. DOI: 10.1002/aenm.201401986.

[40] D. M. Pesko, S. Sawhney, J. Newman, and N. P. Balsara, "Comparing Two Electrochemical Approaches for Measuring Transference Numbers in Concentrated Electrolytes", *J. Electrochem. Soc.*, vol. 165, no. 13, A3014–A3021, Jan. 1, 2018. DOI: 10.1149/2.0231813jes.

[41] A. Ehrl, J. Landesfeind, W. A. Wall, and H. A. Gasteiger, "Determination of Transport Parameters in Liquid Binary Electrolytes: Part II. Transference Number", *J. Electrochem. Soc.*, vol. 164, no. 12, A2716–A2731, Jan. 1, 2017. DOI: 10.1149/2.1681712jes.

[42] G. N. Lewis, "The Theory of the Determination of Transeference Numbers by the Method of Moving Boundaries", *J. Am. Chem. Soc.*, vol. 32, no. 7, pp. 862–869, Jul. 1, 1910. DOI: 10.1021/ja01925a002.

[43] J. Wang, Y. Yamada, K. Sodeyama, C. H. Chiang, Y. Tateyama, and A. Yamada, "Superconcentrated electrolytes for a high-voltage lithium-ion battery", *Nat Commun*, vol. 7, p. 12 032, Jun. 29, 2016. DOI: 10.1038/ncomms12032.

[44] K. Dokko, D. Watanabe, Y. Ugata, M. L. Thomas, S. Tsuzuki, W. Shinoda, K. Hashimoto, K. Ueno, Y. Umebayashi, and M. Watanabe, "Direct Evidence for Li Ion Hopping Conduction in Highly Concentrated Sulfolane-Based Liquid Electrolytes", *J. Phys. Chem. B*, vol. 122, no. 47, pp. 10 736–10 745, Nov. 29, 2018. DOI: 10.1021/acs.jpcb.8b09439.

[45] K. Xu and C. Wang, "Batteries: Widening voltage windows", *Nat. Energy*, vol. 1, no. 10, pp. 1–2, 10 Oct. 6, 2016. DOI: 10.1038/nenergy.2016.161.

[46] W. R. McKinnon and J. R. Dahn, "How to Reduce the Cointercalation of Propylene Carbonate in Li x ZrS2 and Other Layered Compounds", *J. Electrochem. Soc.*, vol. 132, no. 2, pp. 364–366, Jan. 2, 1985. DOI: 10.1149/1.2113839.

[47] S.-K. Jeong, M. Inaba, Y. Iriyama, T. Abe, and Z. Ogumi, "Electrochemical Intercalation of Lithium Ion within Graphite from Propylene Carbonate Solutions", *Electrochem. Solid-State Lett.*, vol. 6, no. 1, A13–A15, Jan. 1, 2003. DOI: 10.1149/1.1526781.

[48] Y. Yamada, K. Furukawa, K. Sodeyama, K. Kikuchi, M. Yaegashi, Y. Tateyama, and A. Yamada, "Unusual Stability of Acetonitrile-Based Superconcentrated Electrolytes for Fast-Charging Lithium-Ion Batteries", *JACS*, vol. 136, no. 13, pp. 5039–5046, Apr. 2, 2014. DOI: 10.1021/ja412807w.

[49] Y. Yamada, Y. Takazawa, K. Miyazaki, and T. Abe, "Electrochemical Lithium Intercalation into Graphite in Dimethyl Sulfoxide-Based Electrolytes: Effect of Solvation Structure of Lithium Ion", *J. Phys. Chem. C*, vol. 114, no. 26, pp. 11 680–11 685, Jul. 8, 2010. DOI: 10.1021/jp1037427.

[50] Y. Yamada, M. Yaegashi, T. Abe, and A. Yamada, "A superconcentrated ether electrolyte for fast-charging Li-ion batteries", *Chem. Commun.*, vol. 49, no. 95, pp. 11 194–11 196, Nov. 5, 2013. DOI: 10.1039/C3CC46665E.

[51] Y. Yamada, K. Usui, C. H. Chiang, K. Kikuchi, K. Furukawa, and A. Yamada, "General Observation of Lithium Intercalation into Graphite in Ethylene-Carbonate-Free Superconcentrated Electrolytes", *ACS Appl. Mater. Interfaces*, vol. 6, no. 14, pp. 10 892–10 899, Jul. 23, 2014. DOI: 10.1021/am5001163.

[52] L. Ma, S. L. Glazier, R. Petibon, J. Xia, J. M. Peters, Q. Liu, J. Allen, R. N. C. Doig, and J. R. Dahn, "A Guide to Ethylene Carbonate-Free Electrolyte Making for Li-Ion Cells", *J. Electrochem. Soc.*, vol. 164, no. 1, A5008–A5018, Jan. 1, 2017. DOI: 10.1149/2.0191701jes.

[53] D. M. Seo, O. Borodin, D. Balogh, M. O'Connell, Q. Ly, S.-D. Han, S. Passerini, and W. A. Henderson, "Electrolyte Solvation and Ionic Association III. Acetonitrile-Lithium Salt Mixtures–Transport Properties", *J. Electrochem. Soc.*, vol. 160, no. 8, A1061–A1070, Jan. 1, 2013. DOI: 10.1149/2.018308jes.

[54] M. Doyle, T. F. Fuller, and J. Newman, "The importance of the lithium ion transference number in lithium/polymer cells", *Electrochimica Acta*, vol. 39, no. 13, pp. 2073–2081, Sep. 1, 1994. DOI: 10.1016/0013-4686(94)85091-7.

[55] S.-K. Jeong, H.-Y. Seo, D.-H. Kim, H.-K. Han, J.-G. Kim, Y. B. Lee, Y. Iriyama, T. Abe, and Z. Ogumi, "Suppression of dendritic lithium formation by using concentrated electrolyte solutions", *Electrochemistry Communications*, vol. 10, no. 4, pp. 635–638, Apr. 2008. DOI: 10.1016/j.elecom.2008.02.006.

[56] L. Suo, Y.-S. Hu, H. Li, M. Armand, and L. Chen, "A new class of Solvent-in-Salt electrolyte for high-energy rechargeable metallic lithium batteries", *Nat. Commun.*, vol. 4, ncomms2513, Feb. 12, 2013. DOI: 10.1038/ncomms2513.

[57] T. Ma, G.-L. Xu, Y. Li, L. Wang, X. He, J. Zheng, J. Liu, M. H. Engelhard, P. Zapol, L. A. Curtiss, J. Jorne, K. Amine, and Z. Chen, "Revisiting the Corrosion of the Aluminum Current Collector in Lithium-Ion Batteries", *J. Phys. Chem. Lett.*, vol. 8, no. 5, pp. 1072–1077, Mar. 2, 2017. DOI: 10.1021/acs.jpclett.6b02933.

[58] D. W. McOwen, D. M. Seo, O. Borodin, J. Vatamanu, P. D. Boyle, and W. A. Henderson, "Concentrated electrolytes: Decrypting electrolyte properties and reassessing Al corrosion mechanisms", *Energy Environ. Sci*, vol. 7, no. 1, pp. 416–426, Dec. 13, 2013. DOI: 10.1039/C3EE42351D.

[59] Y. Yamada, C. H. Chiang, K. Sodeyama, J. Wang, Y. Tateyama, and A. Yamada, "Corrosion Prevention Mechanism of Aluminum Metal in Superconcentrated Electrolytes", *ChemElectroChem*, vol. 2, no. 11, pp. 1687–1694, Nov. 1, 2015. DOI: 10.1002/celc.201500235.

[60] K. Matsumoto, K. Inoue, K. Nakahara, R. Yuge, T. Noguchi, and K. Utsugi, "Suppression of aluminum corrosion by using high concentration LiTFSI electrolyte", *Journal of Power Sources*, vol. 231, pp. 234–238, Supplement C Jun. 1, 2013. DOI: 10.1016/j.jpowsour.2012.12.028.

[61] L. Suo, O. Borodin, T. Gao, M. Olguin, J. Ho, X. Fan, C. Luo, C. Wang, and K. Xu, ""'Water-in-salt" electrolyte enables high-voltage aqueous lithium-ion chemistries", *Science*, vol. 350, no. 6263, pp. 938–943, Nov. 20, 2015. DOI: 10.1126/science.aab1595.

[62] C. Yang, J. Chen, T. Qing, X. Fan, W. Sun, A. von Cresce, M. S. Ding, O. Borodin, J. Vatamanu, M. A. Schroeder, N. Eidson, C. Wang, and K. Xu, "4.0 V Aqueous Li-Ion Batteries", *Joule*, vol. 1, no. 1, pp. 122–132, Sep. 6, 2017. DOI: 10.1016/j.joule.2017.08.009.

[63] D. Reber, R.-S. Kühnel, and C. Battaglia, "High-voltage aqueous supercapacitors based on NaTFSI", *Sustain. Energy Fuels*, vol. 1, no. 10, pp. 2155–2161, 2017. DOI: 10.1039/C7SE00423K.

[64] P. Lannelongue, R. Bouchal, E. Mourad, C. Bodin, M. Olarte, S. le Vot, F. Favier, and O. Fontaine, ""'Water-in-Salt" for Supercapacitors: A Compromise between Voltage, Power Density, Energy Density and Stability", *J. Electrochem. Soc.*, vol. 165, no. 3, A657–A663, Jan. 1, 2018. DOI: 10.1149/2.0951803jes.

[65] I. Rey, P. Johansson, J. Lindgren, J. C. Lassègues, J. Grondin, and L. Servant, "Spectroscopic and Theoretical Study of (CF3SO2)2N- (TFSI-) and (CF3SO2)2NH (HTFSI)", *J. Phys. Chem. A*, vol. 102, no. 19, pp. 3249–3258, May 1, 1998. DOI: 10.1021/jp980375v.

[66] G. Pagès, V. Gilard, R. Martino, and M. Malet-Martino, "Pulsed-field gradient nuclear magnetic resonance measurements (PFG NMR) for diffusion ordered spectroscopy (DOSY) mapping", *Analyst*, vol. 142, no. 20, pp. 3771–3796, Oct. 9, 2017. DOI: 10.1039/C7AN01031A.

[67] A. Savitzky and M. J. E. Golay, "Smoothing and Differentiation of Data by Simplified Least Squares Procedures.", *Anal. Chem.*, vol. 36, no. 8, pp. 1627–1639, Jul. 1, 1964. DOI: 10.1021/ac60214a047.

[68] B. D. Adams, J. Zheng, X. Ren, W. Xu, and J.-G. Zhang, "Accurate Determination of Coulombic Efficiency for Lithium Metal Anodes and Lithium Metal Batteries", *Adv. Energy Mater.*, vol. 8, no. 7, p. 1 702 097, Mar. 1, 2018. DOI: 10.1002/aenm.201702097.

[69] R. Yazami and Y. F. Reynier, "Mechanism of self-discharge in graphite–lithium anode", *Electrochimica Acta*, vol. 47, no. 8, pp. 1217–1223, Feb. 1, 2002. DOI: 10.1016/S0013-4686(01)00827-1.

[70] R. Mogensen, D. Brandell, and R. Younesi, "Solubility of the Solid Electrolyte Interphase (SEI) in Sodium Ion Batteries", *ACS Energy Lett.*, vol. 1, no. 6, pp. 1173–1178, Dec. 9, 2016. DOI: 10.1021/acsenergylett.6b00491.

[71] A. Klein, T. Mayer, A. Thissen, and W. Jaegermann, "Photoelectron Spectroscopy in Materials Science and Physical Chemistry", *Bunsen-Magazin*, no. 10, 2008.

[72] G. Greczynski and L. Hultman, "C 1s Peak of Adventitious Carbon Aligns to the Vacuum Level: Dire Consequences for Material's Bonding Assignment by Photoelectron Spectroscopy", *ChemPhysChem*, vol. 18, no. 12, pp. 1507–1512, 2017. DOI: 10.1002/cphc.201700126.

[73] G. Greczynski and L. Hultman, "Compromising science by ignorant instrument calibration - need to revisit half a century of published XPS data", *Angew. Chem.*, vol. n/a, no. n/a, 2020. DOI: 10.1002/ange.201916000.

[74] K. Sodeyama, Y. Yamada, K. Aikawa, A. Yamada, and Y. Tateyama, "Sacrificial Anion Reduction Mechanism for Electrochemical Stability Improvement in Highly Concentrated Li-Salt Electrolyte", *JPCC*, vol. 118, no. 26, pp. 14 091–14 097, Jul. 3, 2014. DOI: 10.1021/jp501178n.

[75] K. Hayashi, Y. Nemoto, S.-i. Tobishima, and J.-i. Yamaki, "Mixed solvent electrolyte for high voltage lithium metal secondary cells", *Electrochimica Acta*, vol. 44, no. 14, pp. 2337–2344, Mar. 1, 1999. DOI: 10.1016/S0013-4686(98)00374-0.

[76] Y. Liu, D. Lin, Y. Li, G. Chen, A. Pei, O. Nix, Y. Li, and Y. Cui, "Solubility-mediated sustained release enabling nitrate additive in carbonate electrolytes for stable lithium metal anode", *Nat. Commun.*, vol. 9, no. 1, p. 3656, Sep. 7, 2018. DOI: 10.1038/s41467-018-06077-5.

[77] R. Miao, J. Yang, Z. Xu, J. Wang, Y. Nuli, and L. Sun, "A new ether-based electrolyte for dendrite-free lithium-metal based rechargeable batteries", *Sci. Rep.*, vol. 6, no. 1, pp. 1–9, Feb. 16, 2016. DOI: 10.1038/srep21771.

[78] P. Albertus, S. Babinec, S. Litzelman, and A. Newman, "Status and challenges in enabling the lithium metal electrode for high-energy and low-cost rechargeable batteries", *Nat. Energy*, vol. 3, no. 1, p. 16, Jan. 2018. DOI: 10.1038/s41560-017-0047-2.

[79] J. Wang, Y. Yamada, K. Sodeyama, E. Watanabe, K. Takada, Y. Tateyama, and A. Yamada, "Fire-extinguishing organic electrolytes for safe batteries", *Nat Energy*, vol. 3, no. 1, pp. 22–29, Jan. 2018. DOI: 10.1038/s41560-017-0033-8.

[80] J. E. Harlow, X. Ma, J. Li, E. Logan, Y. Liu, N. Zhang, L. Ma, S. L. Glazier, M. M. E. Cormier, M. Genovese, S. Buteau, A. Cameron, J. E. Stark, and J. R. Dahn, "A Wide Range of Testing Results on an Excellent Lithium-Ion Cell Chemistry to be used as Benchmarks for New Battery Technologies", *J. Electrochem. Soc.*, vol. 166, no. 13, A3031–A3044, Jan. 1, 2019. DOI: 10.1149/2.0981913jes.

[81] E. L. Smith, A. P. Abbott, and K. S. Ryder, "Deep Eutectic Solvents (DESs) and Their Applications", *Chem. Rev.*, vol. 114, no. 21, pp. 11 060–11 082, Nov. 12, 2014. DOI: 10.1021/cr300162p.

[82] M. Angell, C.-J. Pan, Y. Rong, C. Yuan, M.-C. Lin, B.-J. Hwang, and H. Dai, "High Coulombic efficiency aluminum-ion battery using an AlCl3-urea ionic liquid analog electrolyte", *PNAS*, vol. 114, no. 5, pp. 834–839, Jan. 31, 2017. DOI: 10.1073/pnas.1619795114. pmid: 28096353.

[83] S. Chen, J. Zheng, D. Mei, K. S. Han, M. H. Engelhard, W. Zhao, W. Xu, J. Liu, and J.-G. Zhang, "High-Voltage Lithium-Metal Batteries Enabled by Localized High-Concentration Electrolytes", *Adv. Mater.*, vol. 30, no. 21, p. 1 706 102, 2018. DOI: 10.1002/adma.201706102.

[84] T. Doi, Y. Shimizu, M. Hashinokuchi, and M. Inaba, "Dilution of Highly Concentrated LiBF4/Propylene Carbonate Electrolyte Solution with Fluoroalkyl Ethers for 5-V LiNi0.5Mn1.5O4 Positive Electrodes", *J. Electrochem. Soc.*, vol. 164, no. 1, A6412–A6416, Jan. 1, 2017. DOI: 10.1149/2.0611701jes.

[85] J. Zheng, S. Chen, W. Zhao, J. Song, M. H. Engelhard, and J.-G. Zhang, "Extremely Stable Sodium Metal Batteries Enabled by Localized High-Concentration Electrolytes", *ACS Energy Lett.*, vol. 3, no. 2, pp. 315–321, Feb. 9, 2018. DOI: 10.1021/acsenergylett.7b01213.

Acta Universitatis Upsaliensis

Digital Comprehensive Summaries of Uppsala Dissertations from the Faculty of Science and Technology 1913

Editor: The Dean of the Faculty of Science and Technology

A doctoral dissertation from the Faculty of Science and Technology, Uppsala University, is usually a summary of a number of papers. A few copies of the complete dissertation are kept at major Swedish research libraries, while the summary alone is distributed internationally through the series Digital Comprehensive Summaries of Uppsala Dissertations from the Faculty of Science and Technology. (Prior to January, 2005, the series was published under the title "Comprehensive Summaries of Uppsala Dissertations from the Faculty of Science and Technology".)

Distribution: publications.uu.se
urn:nbn:se:uu:diva-406483

ACTA
UNIVERSITATIS
UPSALIENSIS
UPPSALA
2020